Redesigning Peppers RNA Imaging System: an Investigation of *In Vivo* and *In Vitro* Performance

Caitlyn Helena Mendik

Defense Date:

April 3, 2023

Department of Biochemistry

University of Colorado at Boulder

Committee Members

Dr. Amy Palmer: Professor and Associate Chair for Undergraduate Affairs of Biochemistry

Thesis Advisor

Dr. Jeffrey Cameron: Assistant Professor of Biochemistry

Honors Council Representative

Dr. JulieMarie Shepherd Macklin: Academic Director of the Presidents Leadership Class

Outside Reader

Table of Contents

Abstract

RNA is a central component of biochemistry as it carries genetic information, has enzymatic activity, mediates protein biodiversity, and supports other cellular functions. Scientists are continually developing new tools for studying RNA and applying it to fields of research such as medicine and molecular biology. RNA imaging provides one avenue for characterizing RNA by looking at trafficking, localization, and lifetime in living cells. Imaging tools have been on the rise in the past 20 years, providing innovative methods for looking at this nucleic acid under a microscope. Peppers is one of these tools designed by Chen et al. at the East China University of Science and Technology. Peppers is an RNA aptamer engineered to bind a fluorescent probe in a stem loop. The 8Peppers aptamer is the optimized form of their probe and is not repeating units of one aptamer, but a long hairpin turn with eight binding spots for probe; this 8Peppers aptamer has been shown to have difficulties folding into native conformation. This paper aims to redesign Peppers RNA imaging system to produce an effective imaging system with enhanced folding capabilities. This paper looks at its *in vitro* capabilities by fluorescence assay of RNA binding to the probe, HBC620. The redesigned Peppers imaging system is further tested by live cell imaging to determine the efficacy of redesigning the structure, stem, and synonymization of non-consequential regions. The experiments did not show an enhanced fluorescence turn-on or folding capabilities of redesigned Peppers compared to Chen's original Peppers imaging system. However, the original Peppers imaging tool did not have reproducible results and illustrated the need for a comprehensive and standardized characterization system for RNA imaging tools to be dependable.

Introduction

RNA: Essential, yet a Mystery

Nucleic acids, carbohydrates, proteins, and lipids are the essential building blocks of cells. These make us what we are and what we interact with. Ribonucleic acid (RNA) is central to these four organic building blocks, by performing functions as a nucleic acid and by encoding for proteins. The central dogma of biology states that deoxyribonucleic acid (DNA) is transcribed into RNA and then RNA is translated into protein (Berg, et al., 2019). Every protein in our body is there because RNA coded for it.

RNA itself is composed of a combination of four nucleotides: guanine, uracil, cytosine, and adenine. These are joined together in a singular phosphate backbone. RNA can fold onto itself to form hairpin turns, kissing-loops, pseudoknots, internal-loops, and more as seen in figure 1 (Berg, et al., 2019). Since RNA is built from nucleotides, it was initially believed that RNA only functioned as a nucleic acid. However the folding abilities and 2' hydroxy group give rise to ribozymes, a molecule where RNA acts as an enzyme. RNA also plays a role in transmitting the genetic material of some viruses and in regulating the cell cycle or genetic expression (Heatherington). Within the medical field, RNA defects can be the cause for chronic and fatal conditions.

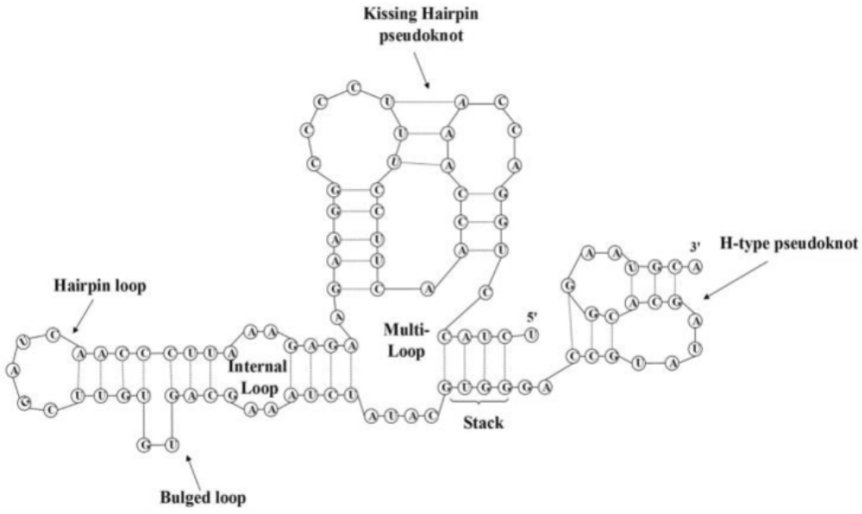

Figure 1: Common RNA folding patterns shown on a RNA. Figure reproduced from Lewis, et al., 2021.

There are multiple types of RNA that have specific functions. These specializations can help with protein synthesis, genetic regulation and editing ("Biochemistry, RNA Structure." NCBI Bookshelf). Here is an abbreviated list of important types of RNA (Berg, et al., 2019):

Name	**Function**
mRNA (messenger RNA)	A RNA that corresponds to the genetic sequence given from DNA. This is the template for making protein with information given from DNA.
rRNA (ribosomal RNA)	A noncoding RNA that binds with ribosomal proteins to make a functional ribosome for translation.
tRNA (transfer RNA)	The bridge between mRNA and protein. An amino acid is attached to the tRNA and the anticodon reads the mRNA to place the correct amino acid on the growing peptide chain.
siRNA (small interfering RNA)	A double stranded RNA that inhibits gene expression by degrading mRNA.
miRNA (micro RNA)	These regulate gene expression by binding to mRNA to repress translation or by binding to promoter regions to upregulate transcription. These are small (21-23 nucleotide) non-coding, single stranded RNA.
snRNA (small nuclear RNA)	These are non-coding RNA that are part of the spliceosome and function to splice introns for making mRNA from pre-mRNA in the nucleus.
ncRNA (non-coding RNA)	A general term for an RNA that is transcribed but does not get turned into protein. Many ncRNAs have functionality in other ways including gene expression regulation and enzymatic activity.

Scientists are just beginning to understand the diversity in structure and function of RNA. Even though many types of RNA have been elucidated, it is difficult to understand what all of

the RNA in a cell does. Of the entire human genome, 80% gets transcribed into RNA. However, only 3% of the genome encodes for proteins. That means that we don't completely understand what 96% of RNA in our cells does (Miller, 2014). With RNA being a key player for medicine and science alike, there is substantial research going into it.

The Field of RNA Research

RNA research falls into two broad categories of answering questions about RNA itself and seeking to apply knowledge of how RNA functions to disease mechanisms and treatments. Some specific active research fields include: explaining pre-mRNA processing, identifying RNA localization within the cell, as well as understanding folding, structure, stability, and RNA-protein interactions. For health-related research, scientists are interested in: the role of RNA in disease, RNA viruses, and RNA-based or targeted therapies ("RNA Biology." National Institutes of Health). This is a heavily abbreviated list with the field of RNA research receiving billions in funding per year.

Recent headlines regarding COVID-19 have shown the importance of this research applied to everyday life. Both the Moderna and Pfizer BioNTech vaccines use mRNA to build your body's defense mechanism against the virus ("How Do Different Types of Covid-19 Vaccines Work?" Mayo Clinic, 2022.). RNA is important as a tool in COVID-19 vaccines and has other applications for chronic conditions such as amyotrophic lateral sclerosis (ALS). New ALS treatments are looking to siRNAs to disrupt commonly mutated genes. Researchers have also found that miRNAs present in the patient's motor neurons can be used for early detection and more advanced ALS screening (Mathias and Le Masson, 2018). RNA metabolism has also been shown to be dysregulated in ALS patients, therefore RNA research has applications in

understanding, diagnosing, and treating ALS (Zaepfel and Rothstein, 2021). The COVID-19 vaccines and ALS applications show the importance of RNA research for clinical applications and improving patient outcomes.

RNA research has promising applications for human health and disease, but scientists wouldn't be able to do this without the development of protocols, tools, and methods for research. There are techniques for purifying, quantifying, synthesizing, and imaging RNA. Each method has its strengths and weaknesses, making it good for specific applications. Improving and diversifying the portfolio of RNA research methods will help other scientists collect higher quality data and be more confident in their conclusions.

Imaging Tools

Microscopy is a key player in RNA research to understand where and when RNA localizes in the cell. Understanding RNA localization is important due to the compartmentalization of cells and importance of local translation. Spatial placement of mRNA can introduce protein gradients, which are important for embryonic development, neuroscience, and more. Temporal control of mRNA also allows proteins to be specifically made for metabolic purposes to modulate cellular equilibrium (Bourke, et al. 2023). Being able to track where and when RNA localizes in the cell is crucial for understanding how cells function. Thus, there is a drive to improve imaging standards and the field of RNA imaging is rapidly growing as new fluorescence imaging systems are being developed.

RNA Imaging Class	Schematic Structure	Explanation
RNA Binding Proteins	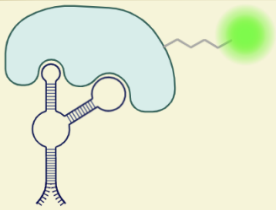	RNA binds protein fused to fluorophore.
Dye Binding Aptamer	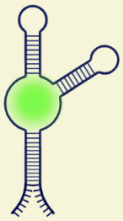	RNA aptamer binds fluorophore and initiates fluorescence turn-on.
CRISPR-Based Systems	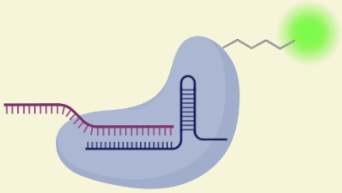	RNA of interested is bound to guide RNA. dCas13 fused to fluorophore is recruited to the RNA of interest.

Figure 2: Overview of main classes of RNA imaging. Figure produced using BioRender.

Imaging systems vary in how the RNA is tagged and by how probes are introduced. Figure 2 describes how classes of RNA imaging systems function. Most RNA imaging methods rely on either fluorescent proteins or fluorescent probes to bind to an RNA element. The RNA element is either genetically encoded or endogenous to the cell. For a protein-binding example, the MS2 system relies on MS2 bacteriophage biology where coat proteins bind to RNA stem loops. The MS2 stem loop is genetically fused to an RNA of interest so the coat protein can bind to this stem loop. The coat proteins have been fused to a fluorescent protein so the RNA can be visualized when the coat protein binds the stem loop.

An example of a small fluorophore probe is the Riboglow system. Riboglow utilizes a naturally occurring cobalamin (vitamin B12) riboswitch to bind to a cobalamin- fluorophore conjugate to initiate fluorescence turn-on. Riboswitches are common mRNA motifs that allow for genetic regulation by binding to small molecules as feedback for expression. Cobalamin

riboswitches bind to vitamin B12 in bacteria to regulate genes involved in vitamin B12 metabolism. This system was harnessed to make an RNA imaging tool. Upon binding, the cobalamin separates to dequench the fluorophore and initiate fluorescence turn-on so the RNA can be visualized (Brasselman, et al. 2020).

The CRISPR-based systems use an endonuclease free Cas13 RNase enzyme to identify and track target RNA. Endogenous RNase, ribonuclease enzyme, cleaves RNA into smaller segments in cells for degradation; the dCas CRISPR system genetically changed the RNase so it can no longer cleave RNA, but can still bind to target RNA via guide RNAs (dCas13). The dCas13 is bound to a fluorophore and the guide RNA is chosen to specifically target an RNA of choice. One pro is that this system doesn't need any genetic modifications to the studied system. The system is limited in that there is not a good standardized approach to creating guide RNA and it has a lower signal-to-noise ratio than the MS2 system (Yang, et al. 2019).

	Tool	Tagging method	Probe introduction	RNA imaged	Single molecule
protein-based	MS2	genetically modified	genetically encoded FP	mRNA ncRNA	X
	PP7	genetically modified	genetically encoded FP	mRNA ncRNA	X
	λN	genetically modified	genetically encoded FP	mRNA	X
	Pepper	genetically modified	genetically encoded FP	mRNA	X
	PUM-HD	endogenous	genetically encoded FP	mRNA ncRNA	X
	dCas13	endogenous	genetically encoded FP	mRNA ncRNA	X
fluorophore-aptamer pair	Spinach, Broccoli, Corn	genetically modified	membrane-permeable dye	mRNA ncRNA	X
	Mango	genetically modified	membrane-permeable dye	mRNA ncRNA	X
	Peppers	genetically modified	membrane-permeable dye	mRNA ncRNA	
dye and quencher	SRB-2	genetically modified	membrane-permeable probe	mRNA ncRNA	X
	RT-aptamer	genetically modified	membrane-permeable probe	mRNA	
	Riboglow	genetically modified	bead-loaded probe	mRNA ncRNA	X[a]
	o-Coral	genetically modified	membrane-permeable probe	mRNA ncRNA	
hybridi-zation	Molecular beacon	endogenous	microinjection or electroporation	mRNA ncRNA	X

[a] Based on results in preprint (Braselmann et al., 2019).

Figure 3: Overview of RNA imaging tools with their respective methods and characteristics. Figure reproduced from Braselmann, et al., 2020.

The current industry standard is the MS2 imaging system. It has been continually modified since its introduction in 1997, but other systems are beginning to challenge its utility (Johansson et al., 2002). New systems include: Riboglow, Peppers, Mango II, biRhoBAST, Spinach2, and more (Braselmann, et al. 2018)(Chen, et al. 2019)(Cawte, et al. 2020)(Bühler, et al. 2021)(Strack, et al. 2015). The tagging method and probe attachment varies between each system. A summary of current RNA imaging systems is presented in Figure 3.

Each system has its pros and cons, giving researchers a selection for imaging RNA in live cells. However, there has not been a consistent and rigorous evaluation of each new system so it is difficult to critically evaluate which system is best for the application. Yet new papers tend to boast that they have the best signal-to-noise ratio and single-molecule sensitivity. Figure 4 shows discrepancies in those declarations as it directly compares the *in vivo* performance of dye binding aptamers. For example, Broccoli-BI and Peppers-HBC620 show only a 1.2-fold fluorescence turn-on which means that the RNA binding the dye shows a minimal increase in brightness when compared to just the dye in non-binding conditions. The biRhoBAST system shows the highest contrast between conditions with and without fluorescent probe. However Bühler reports many of these systems show minimal increase in conditions with the probe, demonstrating a need for further optimization in the performance of many RNA imaging tools. These considerations also only look at performance under a microscope and don't look into transcriptional or translational perturbations.

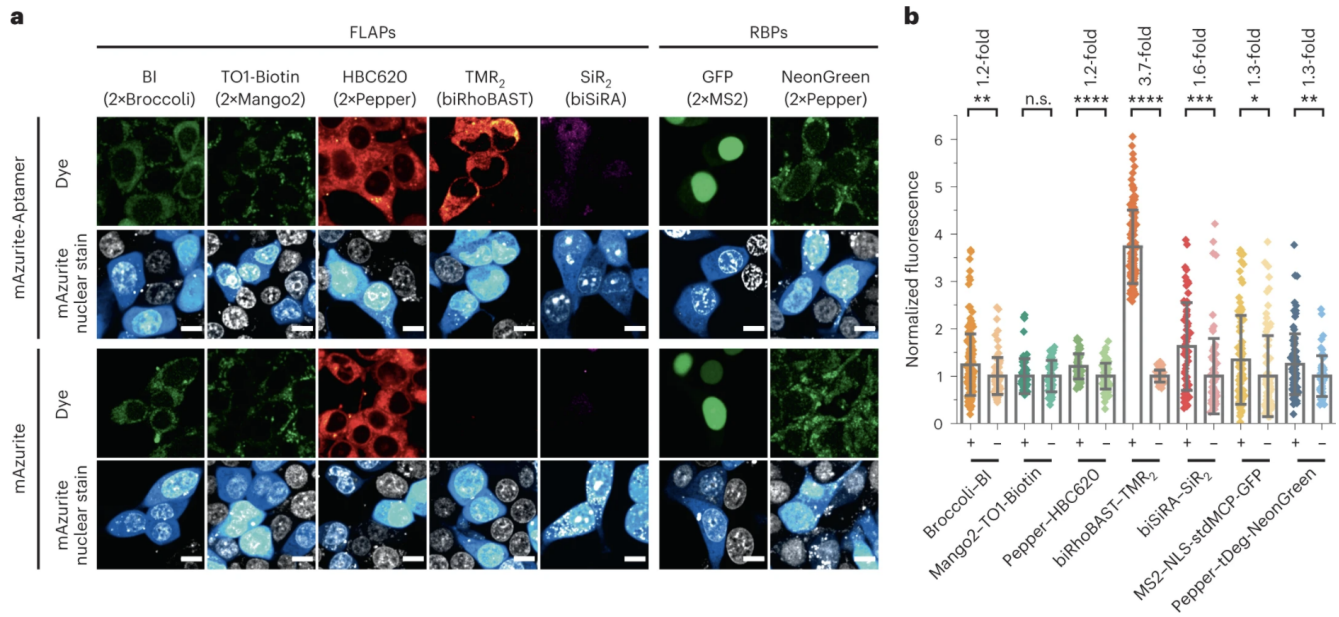

Figure 4: a) Cells expressing mAzurite mRNA that were tagged with two copies of each RNA imaging system. The blue is the nuclear marker and the categories labeled "dye" are showing RNA expression. "FLAP" indicates fluorescent light-up aptamer and "RBP" indicates RNA binding protein. This presents the comparison of images showing the dye and RNA binding (top row) as well as just dye (third row). b) The cytosolic fluorescent intensities of dye and RNA binding compared to just dye. Figure reproduced from Bühler, et al., 2023.

It is possible that introduction of an RNA imaging probe causes the cells to behave differently. For example, it was found that mRNA degradation was inhibited in RNA expressing the MS2 system when tested in yeast. This means introducing the MS2 system caused an accumulation of 3' mRNA fragments because the cell couldn't degrade mRNA fragments bound to MS2 coat proteins (Garcia and Parker, 2015). However, modifications in the MS2 stem loop and MCP protein alleviated this problem (Tutucci, et al., 2018 (1)). This illustrates the importance of testing for cellular perturbation and optimizing the system. Since there is research interest in using RNA imaging tools to track the whole lifespan of mRNA, from transcription through degradation, it is important that the tool does not interfere with this process.

A clear theme in RNA imaging is the importance of single-molecule sensitivity. One of the main uses for RNA imaging is tracking where the RNA moves within the cell and if it colocalizes with other molecules. If single-molecule resolution is not truly achieved, the probe can only give a general overview of where RNA clusters within the cell and doesn't offer precision data. The size of the probe can hinder the movement of the RNA as well. Protein-binding systems, like MS2, tend to be extremely large compared to the actual size of the RNA and perturb its natural activity. The size of the probe can also decrease mRNA stability (Bühler, et al., 2023).

Photostability and phototoxicity of the fluorophore itself can also pose an issue for any type of fluorescence microscopy. Photostabilty refers to the fluorophore's response to light and how long it can maintain its chemical structure upon illumination with light before degrading and losing fluorescence. Phototoxicity is damage to the surrounding cell due to excitation from the lasers used in fluorescence microscopy that can lead to the production of free radicals and oxidative damage. Phototoxicity is also closely linked to photobleaching. When a fluorophore excites, sometimes an electron can go into a triplet state. A triplet state is when an orbital has two unpaired electrons and molecular oxygen is one of the few molecules that has a naturally occurring triplet state. This causes the fluorophore to covalently bind molecular oxygen and the new binding causes one oxygen atom to leave, creating an oxygen radical. The oxygen radical is toxic to the cell and the new covalent bond does irreparable damage to the fluorophore so it no longer emits (Berg, et al., 2019).

In summary, there are many factors involving both the RNA aptamer and fluorescent probe that can pose a challenge to researchers for making a reliable imaging tool. The field would benefit from systematic comparison of the different tools against one another.

Peppers RNA Imaging Tool

Peppers is the name of a fluorescent RNA aptamer designed by scientists at the East China University of Science and Technology. The RNA sequence itself folds into an aptamer that can bind and induce fluorescence-turn on with a fluorescent ligand. It was selected using a technique called systematic evolution of ligands by exponential enrichment (SELEX) against a synthetic dye. In this protocol, the dye, (4-((2-hydroxyethyl)(methyl)amino)-benzylidene)-cyanophenylacetonitrile (HBC) is attached to a column and a library of RNA sequences is washed over in successive rounds to produce an RNA sequence that binds tightly to the HBC dye (Chen, et al., 2019).

Chen and co-workers tested Peppers using multiple different HBC probes and aptamer repeat lengths to optimize the signal-to-noise ratio and fluorescence intensity. Figure 5 shows the chemical structure of each HBC fluorophore named after its emission wavelength, as well as the fluorophore-RNA complex performance *in vitro* and *in vivo*. While all HBC fluorophores showed a fluorescence turn-on using different emission spectrum, HBC620 was found to be the best for live-cell imaging. More specifically, the authors found that HBC620 had the best photostability when compared to other HBC fluorophores using confocal microscopy. The fluorescence intensity followed a slow linear decrease for up to 1000 seconds of exposure (Chen, et al., 2019).

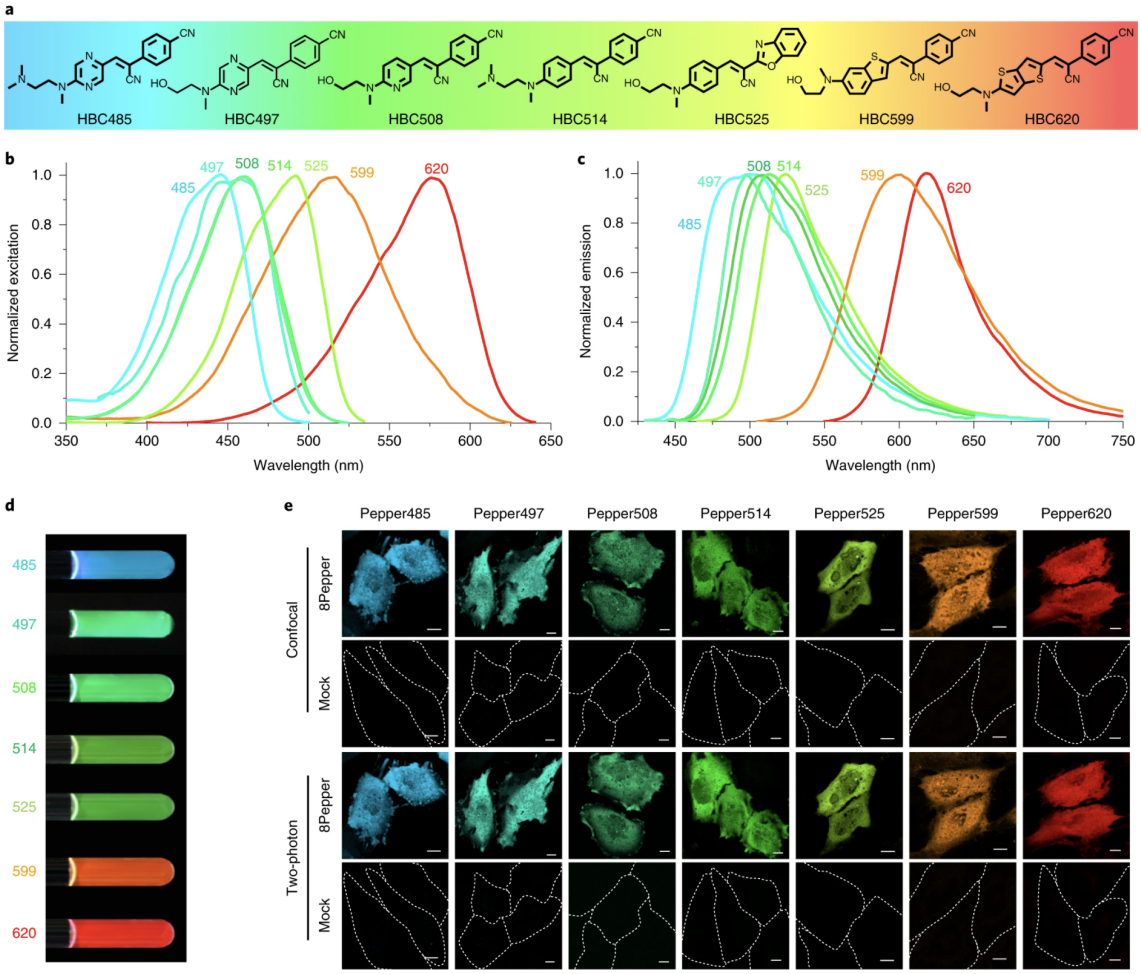

Figure 5: a) The chemical structure of HBC fluorophores. b) The excitation spectrum of each HBC ligand. Excitation wavelength refers to the wavelength of light that causes a fluorochrome to absorb energy from a photon of light. Emission wavelength refers to the wavelength emitted by the energized fluorophore. d) Pepper-fluorophore complexes imaged *in vivo* using UV light. e) Pepper-fluorophore complexes imaged in HeLa cells using confocal and two-photon microscopy. Figure reproduced from Chen, et al., 2019.

When optimizing the repeats of the aptamers, the authors tested two, four, eight, and sixteen Pepper aptamers. Figure 6 shows the predicted folding pattern and in vivo performance of each aptamer array. The authors found that the fluorescence intensity increased up to 8Peppers, followed by diminishing returns for 16Peppers (Chen, et al. 2019).

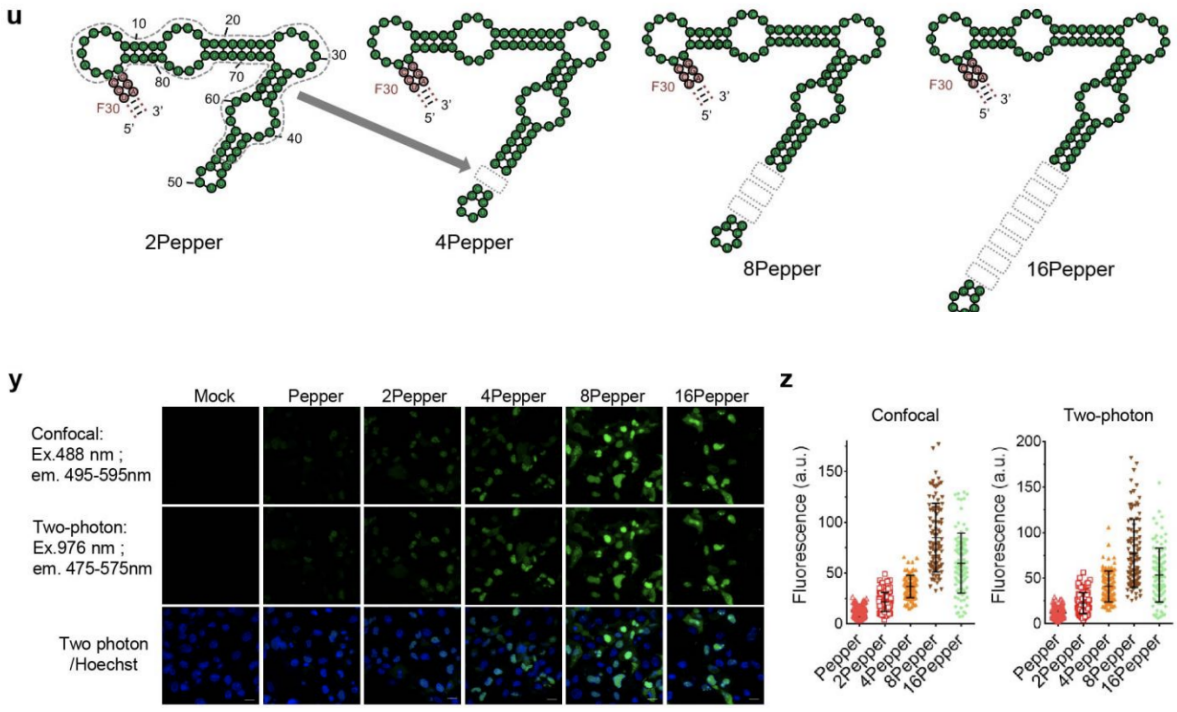

Figure 6: u) The predicted structure of repeating Peppers aptamer. y) Live cell imaging of Peppers in Cos-7 cells. z) Quantitation of cellular fluorescence of each Peppers aptamer. Figure reproduced from Chen, et al. 2019.

Research Objective

Between RNA imaging probe structures, single-molecule sensitivity, cellular and RNA perturbations, and fluorophore performance, there is a lot of variability between each RNA imaging system. A universal system of how to compare the behavior and performance of individual imaging tools has not been established. Graduate student Erin Richards in the Palmer lab is looking to propose a systematic pipeline of characterization for RNA imaging tools.

Richards' system looks at single-molecule resolution, live-cell and fixed cell imaging, transcriptional and translational perturbation, and suggests a universal plasmid layout to insert the genetically encoded RNA element. This would allow different imaging systems to be compared directly to one another and would enable each platform to be tested in a variety of

settings including confocal imaging and single-molecule *in situ* fluorescence hybridization (smFISH).

The two main research objectives of this paper are to test Richards' systematic pipeline of RNA tool evaluation and to optimize the Peppers aptamer. The evaluation of RNA imaging tools includes: live-cell imaging, smFISH, RT-qPCR, western blots, and cloning into the pre-designed plasmid. This allows a thorough evaluation of how the RNA imaging system works in live and fixed cells and if it perturbs function. The RNA imaging system of choice is Peppers.

Here I hoped to optimize 8Peppers and reduce issues with folding. In this paper I will reference the Peppers aptamer created by Chen and co-workers as "wild type Peppers," or "WT Peppers," since it was the original Peppers created. WT 8Peppers folds into a long hairpin turn as shown in figure 7. This unique folding pattern can make it difficult to form the native, folded state *in vitro* and *in vivo.* The process in which RNA goes from a disordered state to its native state involves folding kinetics, thermodynamic stability in base pairing, metal ions, and RNA-binding proteins. The conditions within cells are variable and fluctuations in temperature and metal ion concentration can influence RNA folding into an inactive conformation that becomes rate limiting (Zemora and Waldsich, 2010). Figure 8 shows a visual representation of non-cooperative binding and how it can lead to misfolding (Leamy, et al., 2016).

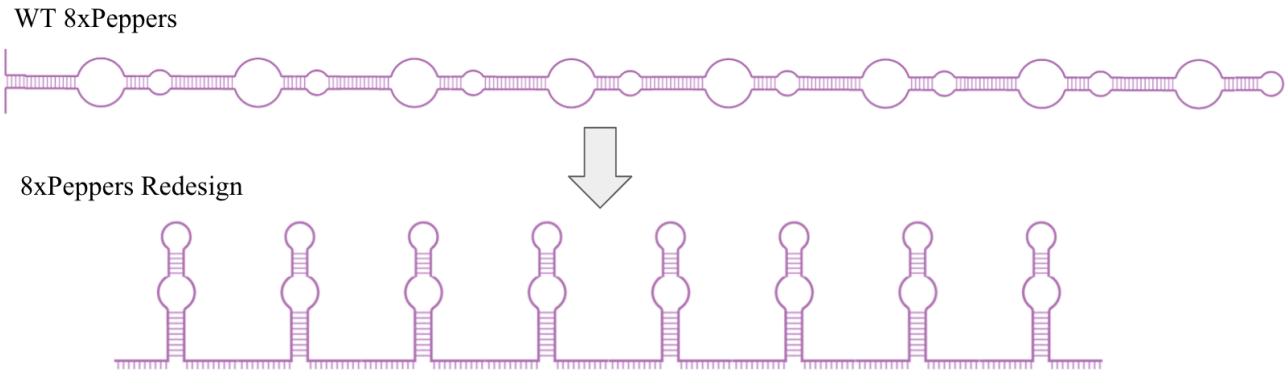

Figure 7: Visual representation of WT 8Peppers in its linear hairpin turn and Redesigned 8Peppers as multiple short hairpin turns separated by a 50 nucleotide linker. The pictured structures don't represent the thermodynamically folded state, but rather show a conceptual representation of the long hairpin versus array of aptamers. Figured produced using Bio Render.

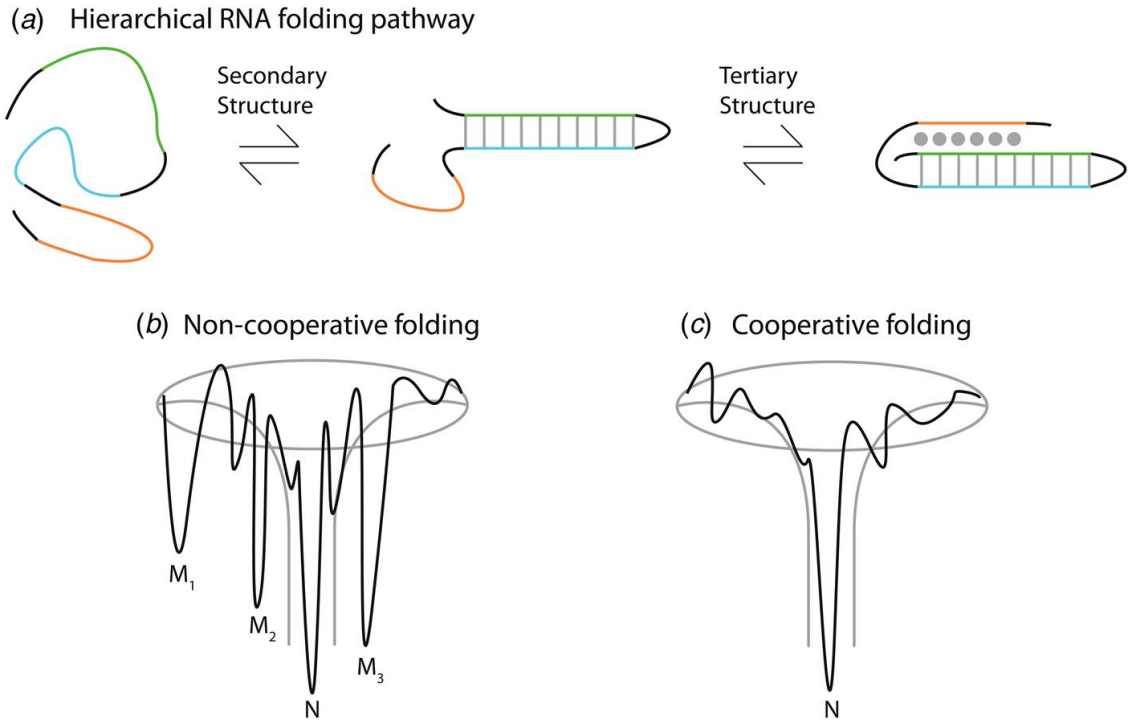

Figure 8: a) The folding pathway of RNA as it base pairs to form a secondary structure and then into tertiary structure influenced by metal ions. b) Free energy diagram of non-cooperative folding where RNA can misfold into non-native conformations, such as M_1, and be "stuck" in that state due to a high activation energy to refold to a native, N, state. The y-axis is

representative of free energy or the work needed to make a change in a thermodynamic system at equilibrium. The x-axis represents folding conformations of the RNA. c) Cooperative folding where intermediates do not pose a large threat to native folding of RNA. Figure reproduced from Leamy, et al., 2016.

Since WT 8Peppers has to wait until the entire sequence has been transcribed to fold properly, it is at high risk of misfolding. In cells, RNA undergoes co-transcriptional folding. In co-transcriptional folding, nascent transcripts fold virtually at the same time they are being transcribed. In order to work around this issue, we are proposing to redesign WT 8Peppers. I speculate that synonymizing the WT 1Pepper and attaching it in a row of eight using nucleotide linkers will allow each Pepper aptamer to fold correctly while still allowing for the same robust signal intensity as WT 8Peppers. Synonymization with nucleic acid means achieving the same folding pattern and function via different nucleotide sequences. Wu and coworkers showed that cells more stably and reproducibly expressed the synonymized sequences as compared to the perfect repeats. This was shown first by synonymizing green fluorescent protein (changing the nucleic acid sequence while preserving the amino acid sequence) and measuring the fluorescence intensity to reveal a better signal-to-noise ratio. They also synonymized the MS2 stem loop to generate a series of non-repetitive sequences by creating complementary mutations in the MS2 stem, while still preserving the ability of the MS2 stem loop to bind MCP. They found that the synonymized sequence had more homogenous expression of the RNA imaging system between cells (Wu, et al, 2015). They speculated that by decreasing repetition, they decreased the propensity of repetitive sequences to recombine and get deleted. With these findings in mind, I mutated each Pepper aptamer to make each one slightly different so they are not perfect repeats.

This paper will explore the redesign of 8Peppers to allow for a more user-friendly folding capability, as well as aiming to validate Erin Richards' systematic pipeline of evaluation for RNA imaging tools.

Methods

Array Design

Designed by Dr. Rob Batey, Dr. Amy Palmer, and Caitlyn Mendik

The 8Peppers array was designed using a single Peppers sequence without the three nucleotide stem (Supplementary Table 1). The sequence was synonymized in two regions: the tetraloop and the stem leading to the tetraloop. The tetraloop was synonymized using UNYG and GNRA patterns following IUPAC codes. The stem was synonymized by randomly changing base pairs to other complementary base pairs as shown in figure 9. This was done to prevent misfolding between Peppers aptamers in the complete array. The eight synonymized Peppers sequences (Supplementary Table 3) were then placed in the MS2V6 array (Vera, et al. 2019).

The MS2V6 system was chosen for its 50 nucleotide linkers in between the repeating MS2 aptamers. MS2V6 was found to outperform MS2V5 and MS2V7 in RNA degradation patterns and brightness (Tutucci, et al., 2018 (1)). We chose to make a construct with 8 Pepper aptamers, because previously it was shown that the 8Peppers construct performed better than two, four, and sixteen Peppers (Chen, et al., 2019).

To insert Peppers, the MS2 loops were deleted starting from the A-bulge through the following sequence: xxANYAxx (Tutucci, et al., 2018 (2)). As shown in figure 9, this left the stem structure to attach the Peppers aptamer. The original stem on the Peppers aptamer was deleted. The synonymized Peppers aptamers were then added in place of the MS2 loops.

Initially the sequence did not fold properly in RNA folding prediction software, so adjustments were made to help promote proper folding in the stem and synonymized Peppers. The array was then ordered as two gBlocks. It was split into two gBlocks because one full gBlock failed the IDT complexity score. However by splitting into two gBlocks, the array could be synthesized without a failing complexity score and then amplified to full length via PCR.

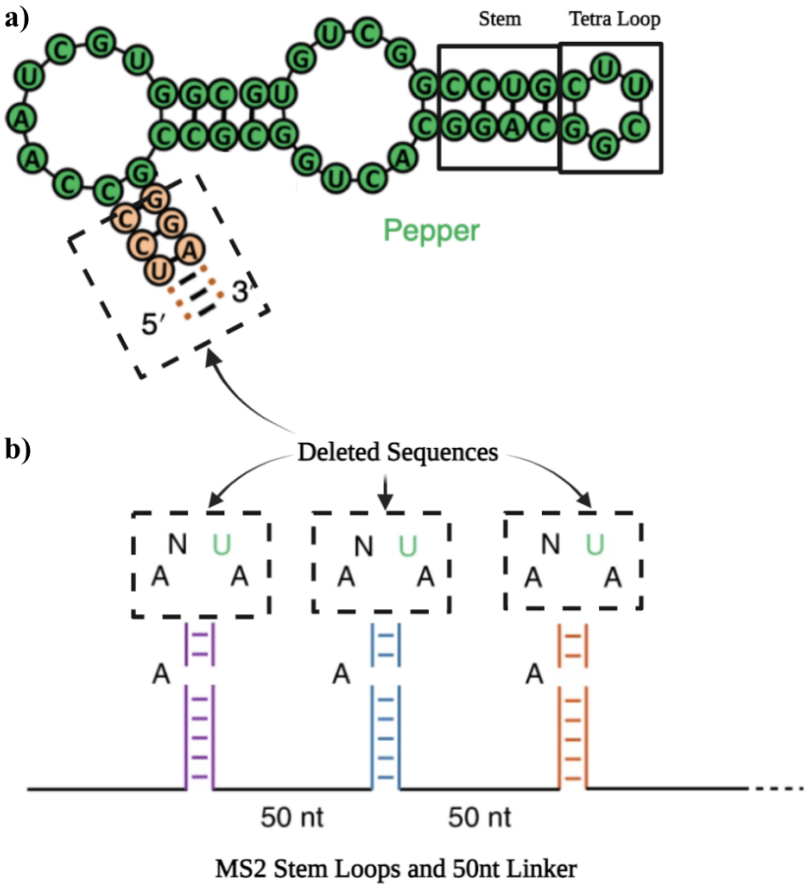

Figure 9: a) Predicted secondary structure of Peppers. Figure reproduced from Chen, et al., 2019 and modified using BioRender. b) MS2 loops with 50 nucleotide linkers showing deleted sequences to create a linker system for redesigned Peppers. Figure reproduced from Tutucci, et al., 2018 (2) and modified using BioRender.

Primer Design

Designed by Dr. Amy Palmer and Dr. Rob Batey

In order to compare the 8Peppers redesign to the original Peppers, we designed primers to *in vitro* transcribe the first, first 4, and first 8 Peppers aptamers of the original Peppers construct. Primers for cloning were designed following Addgene recommendations (How to

Design a Primer). They were chosen with 18-24 base pairs in length, 40%-60% GC content, a melting temperature between 10°C and 15°C, and starting and ending with GC base pairs. All of the primers in the set had melting temperatures within 5℉ of each other and were not complementary. A T7 polymerase binding site was added to the 5' primer so *in vitro* transcription could be done to make the full length RNA. Three 3' primers were designed as reverse complements to the first, fourth, and eighth Peppers array. These were chosen since the array was ordered as two gBlocks and this would allow them to be combined into one array. A GCGC clamp was added to the 5' end of the eighth Peppers primer as well.

A second set of primers were designed after initial *in vitro* experiments to produce WT 1Peppers and redesigned 1Peppers. These primers included only the sequence for the Peppers aptamer with no stem, linkers, or DNA from mammalian expression plasmid. The inner primer included a T7 binding site and included the whole sequence for WT 1Peppers and redesigned 1Peppers. A generic T7 5' primer was used and the 3' primer was designed to anneal to the inner primer. These new primers were created to make *in vitro* folding more effective.

DNA Preparation

The DNA for redesigned 1Peppers, 4Peppers, and 8Peppers had to be synthesized from two gBlocks. PCR was performed using the BIO Rad C1000 Touch Thermal Cycler. Phusion high fidelity polymerase was used because there were many similar repeats within the DNA sequences. The following reagents were added to a thin-walled PCR tube: 10µL 5x Phusion buffer, 1.0 µLPeppers gBlocks (10ng/µL), 0.5 µL Phusion high fidelity polymerase, 2.5 µL forward primer (10nM), 25 µL reverse primer (10nM), 1 uL dNTPs (10mM), and 32.5 µL MilliQ water. When two gBlocks were used, each was added at 0.5 µL for 1.0 µL of total DNA. The

polymerase was added last and PCR tubes were kept on ice while adding reagents. The tubes were briefly centrifuged to ensure all reagents were at the bottom of the tube. If bubbles were present, they were pipetted out.

The thermocycler was set up so it went through an initial denaturing stage at 98℃ for 30 seconds. Then it went through four cycles of: 98℃ for 10 seconds, 55℃ annealing for 30 seconds, and 72℃ extension for 90 seconds. Then the annealing temperature was raised to account for the GC content of the primers. It went through 26 cycles of: 98℃ for 10 seconds, 60℃ annealing for 30 seconds, and 72℃ extension for 90 seconds. A final extension of 72℃ for three and half minutes was done before holding at 4℃. The PCR products were stored in the fridge until later use.

To check the quality of the PCR product, agarose gel electrophoresis was run. A gel was made using 1% ultrapure agarose gel and Tris-Acetate-EDTA (TAE) buffer. Gel red was used to stain the DNA and 1kb plus DNA ladder was used for comparison. The gels were run at 80 volts for about an hour and a half. The gels were visualized using a UV light box. The correct bands were identified based on size and cut out of the gel using a razor. Gel purification was done using Omega Biotech's E.Z.N.A Gel Extraction Kit. The protocol was slightly modified for a longer incubation of the column and eluent in a heat block at 50℃ for 10 minutes. This produced a much higher yield of DNA from the purification. Organic contaminants were minimized by doing two steps of the wash buffer.

The DNA gel purification products were then checked once more on another agarose gel. The DNA for redesigned 1Peppers, 4Peppers, and 8Peppers was stored at -20℃.

Cloning Redesigned 8Peppers into PB-Halo-ACTB-6xA Plasmid

The goal of cloning was to put redesigned 8Peppers into the plasmid Erin Richards' synthesized. The 8Peppers array was put in place of the MS2 or Riboglow array; the plasmid contains puromycin and ampicillin resistance, beta-actin, and HaloTag. Richards' PB-Halo-ACTB-6xA plasmid was digested using AgeI and MluI high fidelity polymerases. Redesigned 8Peppers was also digested with AgeI and MluI. They were incubated at 37℃ for two hours and heat inactivated at 65℃ for 20 minutes. They were then stored at 4℃.

The two products were purified using agarose gel electrophoresis and gel purification with the same protocol outlined above. The digested PB-Halo-ACTB and 8Peppers products were ligated using a T7 DNA ligase. This was done using a one-to-three vector-to-insert molar ratio. The following reagents were added while the tube sat on ice: 10 µL T7 DNA ligase reaction buffer, 1µL T7 DNA ligase, 2.46 µL redesigned 8Peppers, 5 µL digested plasmid, and 1.54 µL nuclease free water. The ligase was added last. The reagents were gently mixed by

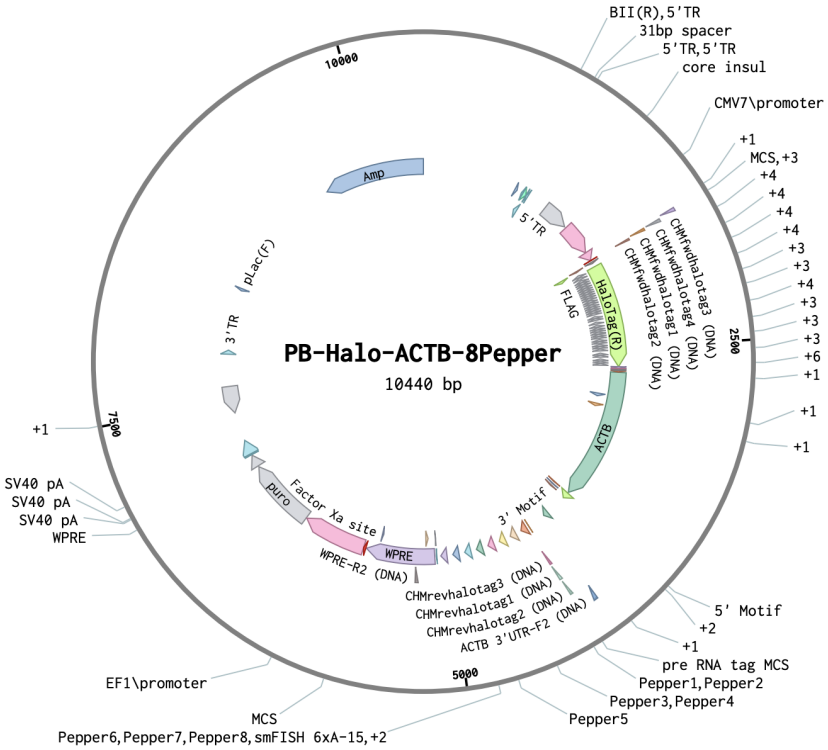

Figure 10: Plasmid map of PB-Halo-ACTB-8Peppers. Each portion of the gene is labeled, for example, HaloTag is shown in green and the ampicillin resistance is shown in blue. Restriction sites are labeled around plasmid. Figure produced from Benchling.com

pipetting, then incubated at room temperature 25°C for 25 minutes. They were put back on ice until transformation into competent cells.

For transformation, the high efficiency transformation for NEB stable competent *E. coli* (C3040H) protocol was followed. 20 uL and 100 uL of the cells transformed with PB-Halo-ACTB-8Peppers were spread onto two separate LB plates supplemented with carbomycin, an ampicillin analog. 100 uL of untransfected cells were spread onto another LB and carbomycin plate. After incubating overnight at 37 C, the untransfected cells did not grow, indicating that the plates and antibiotics were effective. Both plates with the transfected cells showed single colonies.

Individual colonies were chosen and labeled A through F for colony PCR. Colony PCR was done following the CloneAmp HiFi PCR Premix protocol. Each colony was gently streaked from the agar plate using a pipette tip and then mixed into the PCR reaction mix. A control of the undigested plasmid, PB-Halo-ACTB-6xA, was used. Primers from Erin Richards were used to isolate the section that contained either 8Peppers, MS2, or no array. This was chosen because a DNA gel would show if the correct plasmid was made due to the varying length of each array. The thermocycler settings were modified to the following cycle: an initial 95℃ for one minute; then 95℃ for 30 seconds, 55℃ for 30 seconds, and 68℃ for a minute and 30 seconds repeated 29 times; and a final 68℃ extension for five minutes with a 12℃ hold.

The PCR product was then run on agarose gel electrophoresis. 1% Ultrapure gel was used with GeneRuler 1kb Plus DNA Ladder and gel red dye. It was run on 90V for one hour and 22 minutes. The correct length band indicating the presence of redesigned 8Peppers was shown in three of the colonies.

Prior to sequencing, the colonies were miniprepped. Erin Richards performed the mini prep following Omega Biotek's miniprep kit. The following changes were made: after second DNA wash, columns and collection tubes were placed into 70℃ heat block with column tops open for four minutes and then spun down to dry the column; elution buffer was heated to 70℃ and 30 µL put into each column; columns and new 1.7-mL tubes were incubated in 70℃ heat block with column tops closed for five minutes; columns in 1.7-mL tubes spun at 50 xg for 1 min, then at max speed for one minute.

The colonies were sent for sequencing through Plasmidsaurus nanopore sequencing. The sequences were then compared to the predicted sequences for PB-Halo-ACTB-8Peppers. All were within 95% similarity, with the initial colony B showing a 98% similarity. Any base changes from the predicted sequence were in very difficult-to-sequence regions and were anticipated to actually be the desired bases.

The spot for colony B was prepped for use with the Qiagen Midi Prep kit. No changes were made to the protocol. The product was specced using the Denovix DS-11 Spectrophotometer to find the plasmid DNA concentration of PB-Halo-ACTB-8Peppers to be 1300 ng/µL.

Cloning Halo-ACTB into pc-DNA-MCS-Peppers

The protocol for cloning 8Peppers into PB-Halo-ACTB-6xA plasmid was repeated for creating pcDNA-Halo-ACTB-8PeppersWT. Changes included: preparing PB-Halo-ACTB-8Peppers for restriction digest, the enzymes of restriction digest, and which colonies were sent for sequencing. To prepare for restriction digest, I decided on using KpnI and EcoRI because these restriction enzyme sites are present in pc-DNA-MCS-Peppers plasmid and

have a unique sequence from the PB-Halo-ACTB-8Peppers plasmid sequence. I designed primers to lay on either end of the 2600 nucleotide segment that codes for the HaloTag and beta-actin genes in the 8Peppers plasmid. The primers were chosen with 18-24 base pairs in length, 40%-60% GC content, a melting temperature between 10℃ and 15℃, and starting and ending with GC base pairs. The sequence for each KpnI and EcoRI restriction digest enzyme were added to the 5' and 3' primers respectively.

The following reagents were added to a thin-walled PCR tube for PCR: 0.77 µL PB-Halo-ACTB-8Peppers (at 130 ng/µL), 0.5 µL forward primer FwdHaloKnpI (10 nM), 0.5 µL reverse primer RevHaloEcoRI (10 nM), 12.5 µL Clone Amp master mix, and 10.73 µL MilliQ water. The thermocycler was set up so it went through an initial denaturing stage at 95℃ for 3 minutes. Then it went through two cycles of: 95℃ for 30 seconds, 45℃ annealing for 30 seconds, and 68℃ extension for 90 seconds. It went through 31 cycles of: 95℃ for 30 seconds, 58℃ annealing for 30 seconds, and 68℃ extension for 90 seconds. A final extension of 68℃ for five minutes was done before holding at 12℃. The PCR products were stored in the fridge until later use.

The PCR product of HaloTag-ACTB and the pc-DNA-MCS-Peppers plasmid were digested, ligated, and transformed as described above. KpnI and EcoRI restriction digest enzymes were just used instead. Colony PCR with HaloTag specific primers and agarose gels showed that colonies D and E looked like they had the Halo-ACTB sequence. These colonies were miniprepped using E.Z.N.A. Plasmid DNA Mini Kit and no changes were made to the protocol. After sending the sequence to Plasmidsaurus, neither colony had HaloTag-ACTB despite the primers annealing in colony PCR. The ligation, transformation, and colony PCR steps need to be repeated to produce PCSDNA-HaloTag-ACTB-8Peppers.

Preparing HBC620 Stock Solutions

HBC620 was prepared for *in vitro* experiments by dissolving HBC620 powder in 100% anhydrous DMSO (dimethyl sulfoxide) to a final concentration of 1mM. 1mg of HBC620 was dissolved in 2.74 mL DMSO per manufacturer instructions ("HBC620: HBC Analog." Medchemexpress.). The stock solution was stored at -20℃ with no light contact.

HBC620 was prepared for *in vivo* experiments by dissolving HBC620 powder in 10% DMSO, 40% PEG300, 5% Tween-80, and 45% saline. 1mg of HBC620 was dissolved in 100uL DMSO, 400 uL PEG300, 50uL Tween-80, and 450uL saline for a final concentration of 1000uM. The solution was vortexed and sonicated until it was suspended in solution. The stock solution was stored at 20℃ with no light contact.

***In Vitro* Transcription**

Prior to *in vitro* transcription, PCR of the original 1Peppers (Chen, et al., 2019) and redesigned 1Peppers was done. The primers consisted of an internal primer that had just the sequence for each 1Peppers (Supplementary Table 1 and Supplementary Table 3.1) and a T7 binding site. The 5' primer was a general T7 binding sequence and the 3' primer covered the end of the 1Peppers sequences. The following reagents were added to individual PCR tubes: 84µL ddH_2O, 10µL 10x Phusion buffer, 2µL 10 mM dNTPs, 1µL 5' primer (100 µM stock), 1µL 3' primer (100 µM stock), 1µL template (1 µM stock), and 1µL Phusion high fidelity polymerase. PCR was run on a BIO RAD C1000 Touch Thermal Cycler at standard amplification for 2 minutes at 95°C to denature, then 25 cycles of 95°C, 50°C, and 72°C 10 minutes at 72°C to finish with a 16°C hold. The products were checked using a 2% agarose gel with ethidium bromide staining.

For the *in vitro* transcription, the following reagents were added to a conical tube: 62.5µL 10x Transcription buffer, 15µL 1M $MgCl_2$, 5µL 1M DTT, 25 µL 100mM ATP, 25 µL 100mM CTP, 25µL 100mM GTP, 25µL 100mM UTP, 50µL PCR template, 10µL T7 RNA polymerase, 5µL IPP, and 377.5µL ddH_2O. It was then incubated at 37°C for 2.5 hours in a hot water bath. The product was checked using a 12% polyacrylamide gel with urea with a 12.5µL transcription sample and 50µL loading buffer. The product was stored at -20°C.

The RNA was purified by centrifuging the transcription product in a centrifugal filter unit designed to let anything below 10 kDa pass through. It was spun three times with ddH_2O at 10 minutes, 10 minutes, and 20 minute intervals. The concentration and purity of RNA was determined by UV-Vis absorption.

Fluorescence Assay

A fluorescence assay was done to test the fluorescence turn-on of WT 1Peppers and redesigned 1Peppers with HBC620. A 1x buffer was first prepared of 40 mM HEPES at pH 7.0, 100 mM KCl, and 5 mM $MgCl_2$. A 96 well plate was used in the CLARIOstar Plus microplate reader from BMG Labtech. I tested varying concentrations of RNA and probe to see what optimized probe-RNA binding. Technical duplicates were done to increase statistical significance of the following experiment set-ups: 10 nM probe, 10 nM probe and 100 nM WT 1Peppers, 10 nM probe and 100 nM redesigned 1Peppers, 10 nM probe and 500 nM WT 1Peppers, 10 nM probe and 500 nM redesigned 1Peppers, 100 nM probe, 100 nM probe and 100 nM WT 1Peppers, 100 nM probe and 100 nM redesigned 1Peppers, 100 nM probe and 500 nM WT 1Peppers, 100 nM probe and 500 nM redesigned 1Peppers, and buffer only. The samples were

excited at 561 nm and the emission spectrum was measured from 610 to 640 nm wavelength. The intensity was recorded into Excel.

Cell Culture and Passaging

Performed by Erin Richards

U-2 OS cells were obtained from ATCC and maintained in McCoy's 5A supplemented with 10% fetal bovine serum (FBS) and 1% Penicillin/streptomycin (P/S) antibiotics in a humidified incubator at 37°C and 5% CO_2. Cells were rinsed with D-PBS (without Ca^{2+} and Mg^{2+}) before lifting with trypsin-EDTA. Cells were pelleted and resuspended in fresh media to remove excess trypsin-EDTA before plating 1.5 - 2 million cells in 10-cm cell-culture-treated dishes. Over the course of these experiments, cells were passaged each time before reaching total confluency and were free of mycoplasma contamination.

Live Cell Imaging

Media was aspirated off a 10 cm diameter dish of U-2 OS cells from Erin Richards and was washed with 5 mL of D-PBS. The D-PBS was aspirated and replaced with 2 mL of trypsin-EDTA. The cells were incubated with trypsin-EDTA at 37°C and 5% CO_2 for 5 minutes. Once the cells had lifted off the plate and appeared to "waterfall," 4 mL of McCoy's 5A supplemented with 1x P/S and 10% FBS was added. The cells and media were transferred to a 15 mL conical tube and spun for 5 minutes at 300 rcf. The excess media was aspirated off to leave the pellet at the bottom. The pellet was resuspended in 6 mL McCoy's 5A supplemented with 1x P/S and 10% FBS.

A 10 uL aliquot was taken for counting cells. Cells were counted on a Countess II Automated Cell Counter from Thermo Fisher Scientific and 250,000 cells were plated onto homemade 3.5 cm diameter imaging dishes with a glass coverslip bottom. 2 mL of McCoy's 5A supplemented with 1x P/S and 10% FBS was also added to the imaging dishes. These dishes were incubated overnight at 37°C, 80% humidity, and 5% CO_2.

After incubation, cells were transfected with plasmids. Two dishes were made for each construct: LV-HaloTag-ACTB-24xMBSV5, pcDNA-mcs-8PeppersWT with Dendra2-Lifeact-7, and PB-HaloTag-ACTB-8Peppers. The Mirus TransIT-LT1 Transfection Reagent Protocol was followed so 2500 ng of DNA, 250 µL Optimem, and 7.5 µL Transit were incubated at room temperature for 30 minutes before adding to the cells. For the positive control, a 1:2 ratio was done for the plasmid of interest to the transfection marker; the Dendra2-Lifeact-7 plasmid was used as a transfection marker since cloning had failed to produce a WT 8Peppers plasmid with HaloTag-ACTB. This allowed a cytosolic marker for transfected cells. The media was also exchanged for 2 mL of fresh McCoy's 5A supplemented with 1x P/S and 10% FBS. Once the transfection mixture was added, 2µL of JF646-HaloTag ligand was added to each dish that had HaloTag. The dishes were incubated for 48 hours at 37°C, 80% humidity, and 5% CO_2.

For the day of imaging, the imaging dishes were stained one at a time prior to imaging. The media was aspirated and 1 mL of FluoroBrite-DMEM supplemented with 10% FBS was added. Two drops of NucBlu were added and the plates were incubated for 30 minutes at 37°C, 80% humidity, and 5% CO. The media and NucBlu were aspirated and replaced with 1 mL FluoroBrite-DMEM supplemented with 10% FBS. 1 µM HBC620 was present in the media during imaging. This was repeated so the imaging dish was ready for imaging right when it went on the microscope to minimize cellular perturbation from NucBlu.

Images were taken on a Nikon Spinning Disk Confocal microscope. The 20x 0.75 NA air objective and an Excelitas X-Cite 120LED Boost light source were used. An Andor iXon Ultra 888 camera recorded data. An Okolab Cage Incubator kept the environment at 37°C and 5% CO_2. Images were manually taken by searching for fields of view with cells expressing the array. Cells expressing the MS2 and redesigned 8Peppers array were identified by JF646-HaloTag fluorescence using the reasoning that if the cells contain the plasmid expressing the RNA, they will also make the HaloTag-beta-actin protein, which is labeled with JF646. Cells expressing the WT 8Peppers array were identified by Dendra2-GFP fluorescence using the reasoning that if the cell had uptaken the Dendra2-LifeAct-7 plasmid, it was also expressing WT 8Peppers.

A 3-plane z-stack was taken 0.6 µm apart and focused in the middle of the cell with an 800 x 1000 pixel region of interest and no binning. Images were taken in four channels with the following information:

Channel (nm)	**Filter Set (nm)**	**Laser Power (percent)**	**Exposure (ms)**	**Target**
405	428-466	20	300	NucBlu
640	671-739	15	500	HaloTag-JF646
561	590-650	15	300	WT 8Peppers and Redesigned 8Peppers
488	500-550	7-15	300	Dendra2

Data were recorded by Nikon Elements v5.30 and stored in the Palmer Lab group remote server.

Image Analysis

Protocol from Erin Richards

The images were analyzed in FIJI/ImageJ and a custom MATLAB script. Briefly, transfected cells were found in the HaloTag-JF646 or Dendra2-GFP channel and outlined with the polygon selection tool. A mask was created with the FIJI "Selection" --> "Create Mask" tool and saved as a .tif file. The .nd2 image files and the .tif cell masks were imported into the custom MATLAB script and separated into image channels. The HBC620 channel was a maximum intensity projection and the mean and median HBC620 channel pixel intensity were recorded for each masked cell. By graphing pixel intensity versus count, we determined that median intensity was a more fair representation of the data, as most cells had a small amount of very bright pixels in the HBC620 channel. The median HBC620 pixel intensity in each cell was saved under its construct and condition. The pixel intensities were exported into an Excel spreadsheet. These values were then imported into GraphPad Prism 9 to create a column graph where each column was a construct and condition. The construct and conditions were compared with a one-way ANOVA Kruskal-Wallis test for non-parametric data. The values were plotted with each cell represented as a marker, middle bar representing the mean for that construct and condition, and the error bars as the standard deviation. The custom MATLAB script can be found at github.com/erin-m-richards/imaging-tools as WholeCellFluorescence.mlx.

Materials

Reagent	Use	Source	Notes
8Pepper-block1	gBlock DNA	IDT Batch #: 508456667 Ref #: 417834420	
8Pepper-block2	gBlock DNA	IDT Batch #: 508456680 Ref #: 417834421	
5Pepper array t7 fwd	Forward Primer	IDT Batch #: 507911205 Ref #: 417834424	GCGGCCTAATACG ACTCACTATAGGG AGA ACCGGTAACCTAC AAGCTCAGC
3Pepper1 rev	Reverse Primer	IDT Batch #: 507752723 Ref #: 417834425	CATGCCGATATTC TGCACCATGC
3Pepper4 rev	Reverse Primer	IDT Batch #: 507752724 Ref #: 417834426	CTTTGCATGGGTT GGTTGACAGAG
3Pepper8 rev	Reverse Primer	IDT Batch #: 507752831 Ref #: 417834427	GCGCACGCGTATG AGATCTCGTGTGA GG
dNTPs	Reagent	New England BioLabs	
Phusion High-Fidelity DNA Polymerase	Enzyme	New England BioLabs	
5x Phusion HF Buffer	Buffer	New England BioLabs	
Ultrapure Agarose Gel	Reagent	Sigma Aldrich	
GeneRuler 1kb Plus DNA Ladder	Reagent	Thermo Scientific	

Red Loading Dye	Reagent	Thermo Scientific	
Tris-Acetate-EDTA (TAE)	Buffer	Sigma Aldrich	40 mM Tris, 20 mM acetic acid, and 0.4 mM EDTA
Nucleospin Gel and PCR Clean-up	DNA Extraction Kit	Machery-Nagel	
AgeI-HF	Restriction Digest Enzyme	New England Biolabs	
MluI-HF	Restriction Digest Enzyme	New England Biolabs	
CutSmart	Buffer	New England Biolabs	
E.Z.N.A Gel Extraction Kit	DNA Extraction Kit	Omega Biotech	
E.Z.N.A. Cycle Pure Clean-Up Kit	PCR Clean Up Kit	Omega Biotech	
PB-Halo-ACTB-6xA	Plasmid	Erin Richards	PiggyBac Plasmid with HaloTag, 6xA MS2, beta-actin, and ampicillin resistance
T7 DNA Ligase	Enzyme	New England Biolabs	
T7 DNA Ligase Buffer	Buffer	New England Biolabs	
E. Coli C3040H	Competent Cells	New England Biolabs	
10-beta/Stable Outgrowth Medium	Medium	New England Biolabs	
ACTB 3'UTR-F2	Primer	Erin Richards	CCATGAAATAAGT GGTTACAGGAAG
WPRE-R2	Primer	Erin Richards	GCAACCAGGATTT ATACAAGGAGG
CloneAmp HiFi PCR PreMix	Buffer and Enzyme PCR Mix	Takara Bio Company	
Omega Biotek Miniprep Kit	MiniPrep	Omega Biotek	

Lysogeny Broth (LB)	Growth Medium	Palmer Lab	
Carbenicillin (Amp)	Antibiotic	GoldBio	
RedesignedFwd	Primer	IDT Batch #: 520497539 Ref #: 425669699	GCGGCCTAATACG ACTCACTATAGGG AGACATGCGCAAT CGTGCGGTGTCG GTCTGCGCGAGC AGACACTGGCCG CCGCATG
RedesignedRev	Primer	IDT Batch #: 520322532 Ref #: 425669700	CATGCGGCGGCC AGTGTCTGCTCGC GC
WTPepperFwd	Primer	IDT Batch #: 520497538 Ref #: 425669701	GCGGCCTAATACG ACTCACTATAGGG AGAGGCTCCCCA ATCGTGGCGTGTC GGCCTGCTTCGGC AGGCACTGGCGC CGGGAGCC
WTPepperRev	Primer	IDT Batch #: 520296671 Ref #: 425669702	TGGCTCCCGGCGC CAGTGCCCTG
10x Transcription Buffer	Buffer	Batey Lab	
2M $MgCl_2$	Reagent	Batey Lab	
Dithiothreitol (DTT)	Reducing Reagent	Batey Lab	
rATP	Reagent	Batey Lab	
rCTP	Reagent	Batey Lab	
rGTP	Reagent	Batey Lab	
rUTP	Reagent	Batey Lab	
T7 RNA Polymerase	Enzyme	Batey Lab	
Inositol polyphosphate-1-phosphatase (IPPase)	Enzyme	Batey Lab	

Acrylamide	Reagent	Batey Lab	
8M Urea TAE Diluent	Reagent	Batey Lab	
Tetramethylethylenediamine (TEMED)	Reagent	Batey Lab	
Ammonium Persulfate (APS)	Reagent	Batey Lab	
Bromophenol Blue–Xylene Cyanol Dye solution	Reagent	Batey Lab	
Tris/Borate/EDTA Buffer (TBE)	Buffer	Batey Lab	45mM Tris, 45mM Boric Acid, 1mM EDTA
Ethidium Bromide	Reagent	Batey Lab	
Quick-Loading Purple 1kb Plus DNA Ladder	Reagent	Batey Lab	
Gel Loading Purple (6x)	Reagent	Batey Lab	
QIAGEN Plasmid Midi Prep	Kit	QIAGEN	
HBC620	Fluorophore	1.FR BioTechnology 2.MedChem Express	1. Courtesy of Dr. Jeff Cameron 2.Palmer Lab
Human Bone Osteosarcoma Epithelial (U-2 OS) Cells	Cell Line	ATCC	HTB-96
Phosphate Buffered Saline (PBS)	Buffer	Cell Culture Core Facility	137 mM NaCl, 2.7 mM KCl, 8 mM Na_2HPO_4, and 2 mM KH_2PO_4
Trypsin-EDTA	Reagent	Fisher Scientific	
McCoys 5A Media	Media	Cell Culture Core	

		Facility	
Opti-MEM	Reagent	Thermofischer	
TransIT-LT1	Reagent	Mirus	
PB-Halo-ACTB-24x Syn	Plasmid	Erin Richards	PiggyBac Plasmid with HaloTag, 24x MS2, beta-actin, and ampicillin resistance
NucBlue	Dye	Thermofischer	
Flourobrite-Dulbeco's Modified Eagle's Medium (DMEM)	Media	Cell Culture Core Facility	
JF 646-HaloTag ligand	Dye	Promega	
40 mM HEPES, pH 7.0 100 mM KCl, 5 mM MgCl2	Buffer	Caitlyn Mendik	Reagents supplied by Batey Lab
Ultra-15 Centrifugal Filter Unit	Filter	Amicon	Supplied by Batey Lab
HalotagFWDKpnI	Primer	IDT Batch #: 530437507 Ref #: 431606653	GAAGGTACCGATTCTAGAAATCCTGCAG
HalotagRevEcoRI	Primer	IDT Batch #:530437508 Ref #:431606654	GATTAGAATTCGAGCTTGTAGGTTACC
PB-Halo-ACTB-8Peppers	Plasmid	Caitlyn Mendik	PiggyBac Plasmid with HaloTag, 8x peppers redesigned, beta-actin, and ampicillin resistance
pc-DNA-MCS-Pepper	Plasmid	FR Biotechnology	Ampicillin resistance, 8Peppers WT, multiple cloning site
Tween-80	Reagent	Carr, Randolph, and Schwartz Lab	

PEG-300	Reagent	Leinwand Lab	
Dendra2-Lifeact-7	Plasmid	Alex Whiteley Lab	Courtesy of Will Campodonico

Software	**Use**	**Publisher**
RNA Fold	Array structure check	University of Vienna
Fiji	Image Analysis	ImageJ
Benchling	Digital Lab Notebook	Benchling
GraphPad	Data Analysis	GraphPad Software

Results

Workflow

The aim of the experiments was initially to validate Erin Richards' systematic pipeline for evaluating RNA imaging tools and to create a new Peppers aptamer that would have enhanced folding capabilities *in vitro* and *in vivo*. The process was more involved and required time for cloning the DNA for *in vivo* experiments and creating RNA for *in vitro* experiments. A workflow schematic of the completed experiments is shown in figure #. After issues with the initial *in vivo* and in *vitro* experiments, I refined the primer design, got a positive control, and acquired a stock solution of new HBC620. This workflow allowed us to test redesigned Peppers against a negative control and the original WT Peppers, with confidence in our probe and methodology.

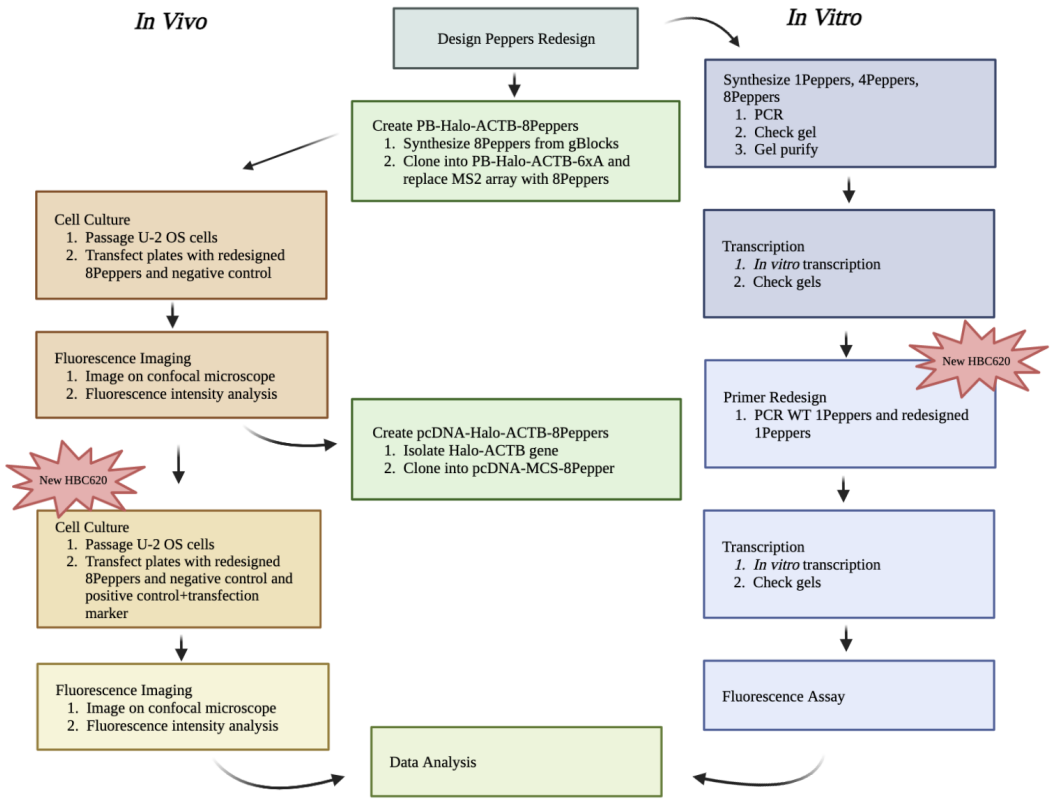

Figure 11: Workflow schematic of major experiments. Figure produced using BioRender.

In Vitro Experiments

The goal of *in vitro* experiments was to test whether the redesigned Pepper arrays could be in vitro transcribed and to test whether the redesigned Peppers aptamers bound the probe and elicited fluorescence turn on. The 8Pepper array was ordered as two gBlocks that could be combined by PCR. I also generated reverse primers that would allow for amplification of the 1st Pepper aptamer only (1Pepper), the first 4 Pepper aptamers (4Pepper) and the full 8 aptamer redesign (8Pepper). After generating cDNA of 1Peppers, 4Peppers, and 8Peppers by PCRs, I performed *in vitro* transcription and used a denaturing gel to assess the lengths of RNA products. Figure 12 shows one of the two denaturing gels under UV shadowing. The denaturing gel disrupts the RNA folding and separates the products by length. This gel confirmed I had made RNA, but the products of the *in vitro* transcription showed RNA of varying lengths. After cutting the bands from the gel and gel purifying the RNA, I ran a 1% agarose gel stained with ethidium bromide to compare the size of the products. This gel confirmed I produced and isolated 1Peppers and 4Peppers RNA. However, 8Peppers RNA was not present. I had difficulty producing the 8Peppers DNA as well, so I had to change directions with the *in vitro* experiments.

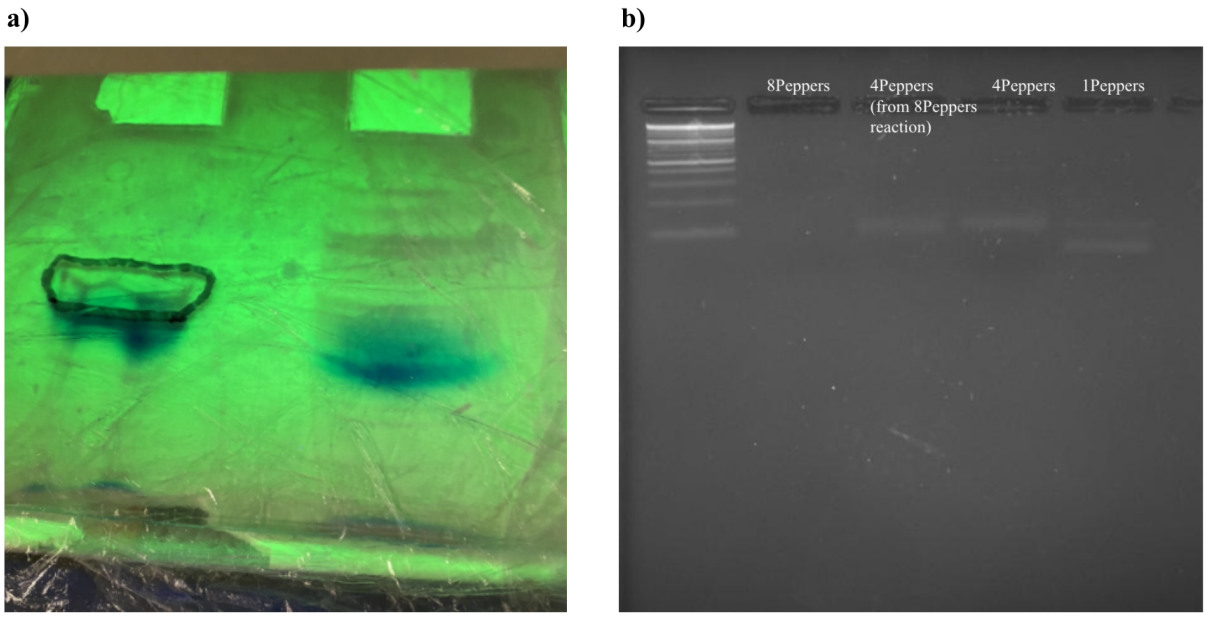

Figure 12: a) A 12% polyacrylamide gel with urea to check the length of RNA products. The denaturing gel electrophoresis showed bands (in blue and circled in black) that were close to the anticipated length of redesigned 8Peppers (left), 4Peppers (right), and 1Peppers (not pictured). These bands were cut and gel purified to obtain the desired RNA based on length. b) A 1% agarose gel stained with ethidium bromide to look at the RNA products of gel clean-up from the denaturing gel showed that redesigned 8Peppers was not present. However RNA of a similar length to 4Peppers and 1Peppers were present.

To troubleshoot, I checked the 1Peppers aptamer using the RNAfold web server from the University of Vienna. The primers initially used contained some of the information needed for the mammalian expression plasmid and the 50 nucleotide linkers. In the folding prediction software, this caused the RNA to misfold as seen in figure 13. Thus, the primers were redesigned to only include the sequence for 1Peppers as outlined in the methods. This produced a predicted folding structure similar to what was anticipated and showed regions where HBC620 could bind.

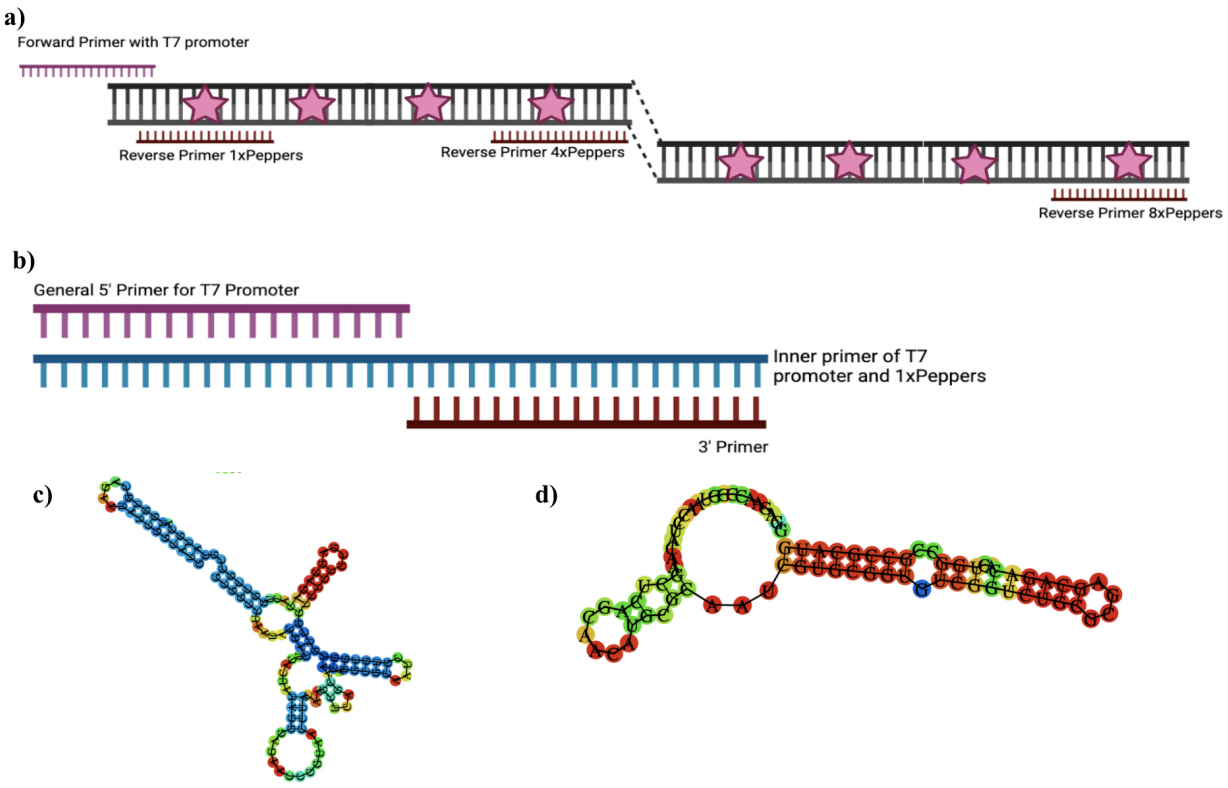

Figure 13: a) Cartoon representation of two gBlocks with initial primers to create Peppers array of varying repeat lengths. These primers include parts of linkers and DNA necessary for cloning into mammalian plasmid. b) Representation of 1Peppers creation with inner primer that included only the sequence for WT 1Peppers or redesigned 1Peppers. c) Predicted folding structure of 1Peppers using the initial primers and d) predicted folding structure of 1Peppers using inner primer set-up. Figure produced using BioRender and folding predictions courtesy of RNA Fold.

Using the new primers, I created WT 1Peppers and redesigned 1Peppers. WT 1Peppers provided a positive control. After PCR, a 1% agarose gel was run as shown in figure 14. There were clear bands present, indicating the PCR produced only the DNA necessary for WT and redesigned 1Peppers. I could then move forward with *in vitro* transcription of the PCR product. I ran another denaturing gel with a sample of the transcription product as shown in figure 14. This gel shows other RNA products made and salts from the transcription buffer, which accounts for the visually long bands. The brightest part of the band shows the main product and this correlates

with the anticipated band length for WT and redesigned 1Peppers, confirming the RNA was produced. The WT 1Peppers band was brighter, indicating it had more RNA product.

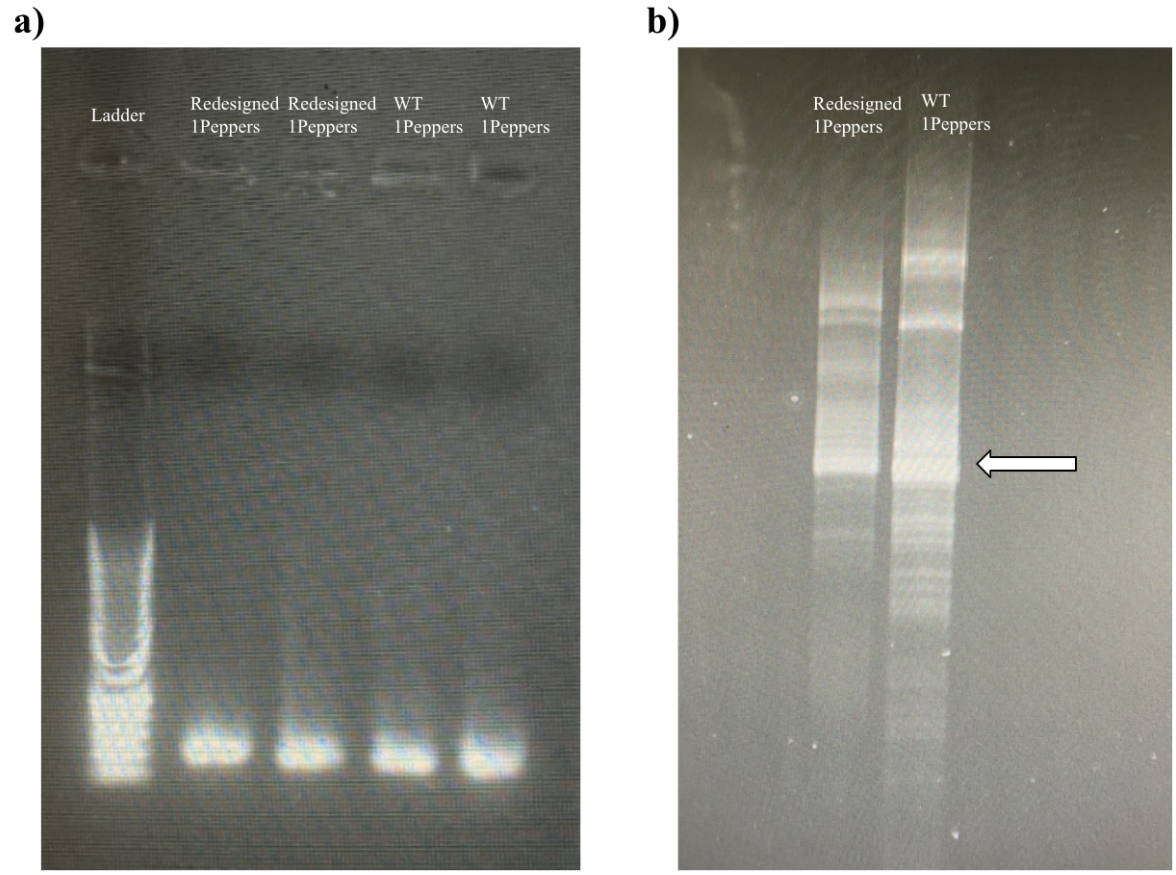

Figure 14: a) A 1% agarose gel stained with ethidium bromide to check the PCR products of WT 1Peppers and Redesigned 1Peppers. b) A 12% polyacrylamide gel with urea and stained with ethidium bromide shows the in vitro transcription products. The arrow indicates the desired product size. The intensity of the band correlates to the amount of product made.

The transcription reaction was purified and the RNA concentration was determined for the fluorescence assay. Figure 15 shows the results of the fluorescence assay. The background fluorescence was determined by combining probe and buffer for each probe concentration. This background was subtracted from each experimental value to give only the fluorescence intensity

due to RNA binding; the intensity was integrated over the whole emission spectrum of HBC620. Technical duplicates are plotted with the mean and standard deviation.

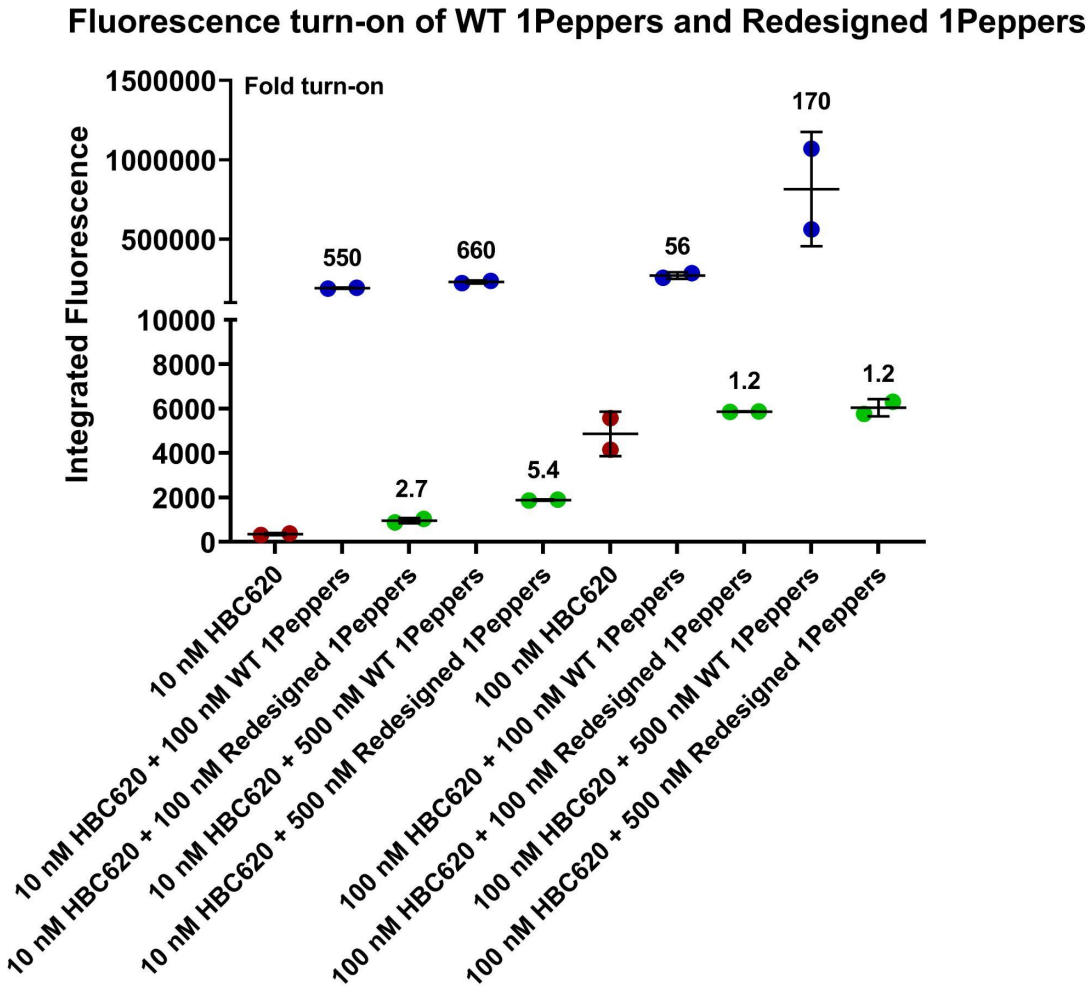

Figure 15: The integrated fluorescence intensity of HBC620 turn-on when bound to WT 1Peppers (blue) and redesigned 1Peppers (green). The probe is tested at 10 nM and 100 nM concentrations and the RNA is tested at 100 nM and 500 nM concentrations. Fold-turn on shows how much higher the fluorescence intensity is than the background of buffer and probe only (red).

The fluorescence intensity for both the WT and redesigned 1Peppers is dependent on probe concentration. When probe concentration increases from 10 nM to 100 nM the fold-turn

on decreases, however, the fluorescence intensity increases for both WT and redesigned 1Pepper. This could be due to an increase in background intensity when more probe is in solution. Increasing the RNA concentration does not have as big of an effect, although the fold-turn on does increase for each condition, with the exception of 100 nM probe and redesigned 1Peppers. There is more RNA in solution to bind the probe, but it might not be effectively binding the probe to produce a more dramatic fluorescence intensity increase.

WT 1Peppers induces a significantly higher fluorescence turn-on than redesigned 1Peppers. For conditions with 10nM probe, the WT 1Peppers was 203 times brighter than redesigned 1Peppers at 100 mM RNA and 122 times brighter at 500 nM RNA. This indicates the WT 1Peppers binds HBC620 more effectively to initiate fluorescence turn-on.

In Vivo Experiments

Redesigned 8Peppers was tested by live cell imaging in U-2 OS cells to measure its performance binding HBC620. An MS2 array was used as the negative control because it should not bind HBC620. WT 8Peppers was used as a positive control to compare to redesigned 8Peppers' fluorescence turn-on. For the first imaging experiment, redesigned 8Peppers was compared only to the MS2 system as the negative control. There was minimal fluorescence-turn on with redesigned 8Peppers, so a second experiment was repeated with a positive control and new HBC620 stock solution.

Cells were transfected with LV-HaloTag-ACTB-24xMBSV5 or PB-HaloTag-ACTB-8Peppers, stained with HBC620 probe, and imaged on a widefield fluorescence microscope. Figure 16 shows the image analysis method. The HaloTag-JF646 channel was used to identify transfected cells. Transfected cells were outlined and subsequently

the field of view was visualized in the HBC620 channel. There was not a clear visual difference between the HBC620 channel when probe was added or not added. I would have predicted that if 8Pepper could bind HBC620, cells expressing this construct (hence HaloTag JF-646 positive cells, those outlined in images in Figure 16) would exhibit higher fluorescence intensity in the HBC620 channel.

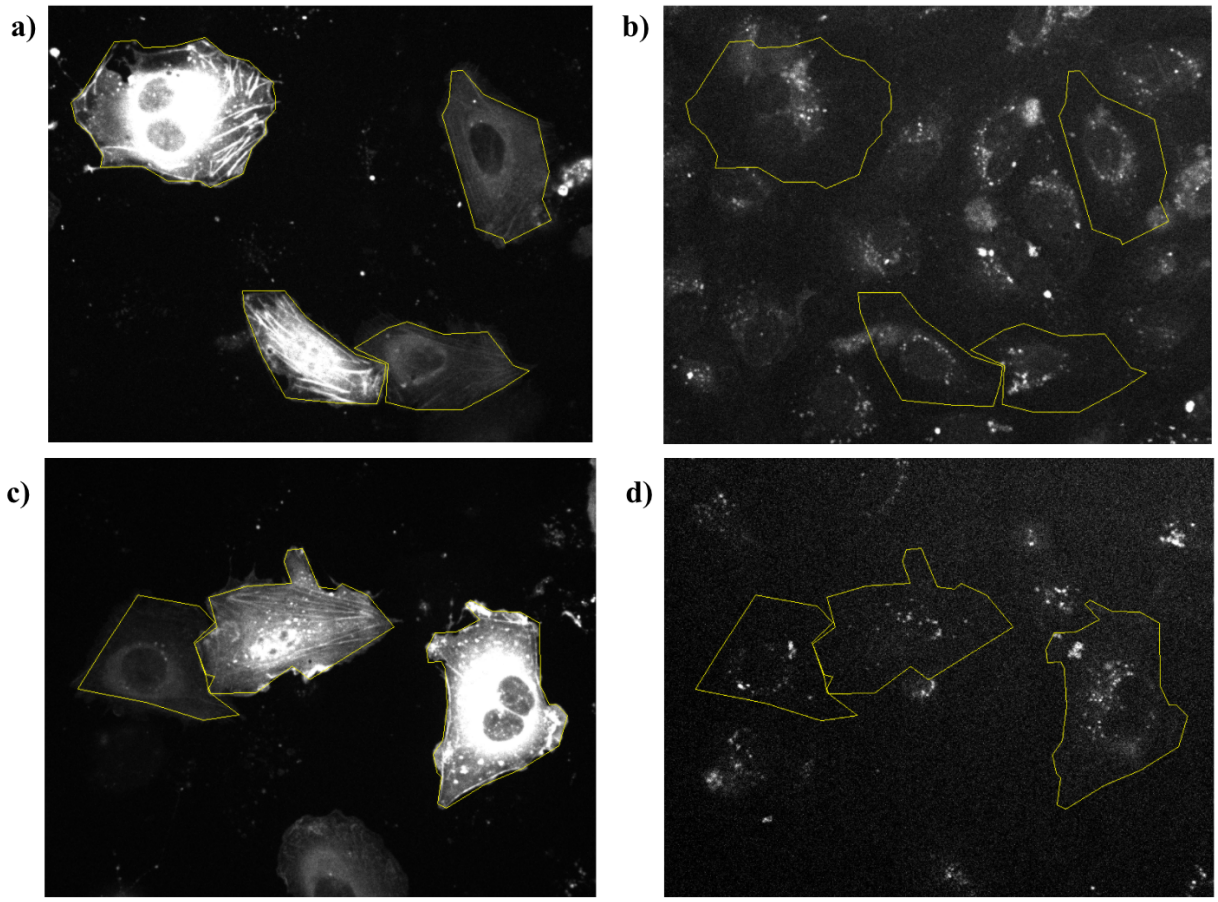

Figure 16: a and b) Cells transfected with PB-Halo-ACTB-8Peppers and 1 μM HBC620 added. a) The HaloTag- JF646 channel is shown with transfected cells masked. b) The HBC620 channel is shown with transfected cells masked. c and d) Cells transfected with PB-Halo-ACTB-8Peppers and no probe. c) The HaloTag- JF646 channel is shown with transfected cells masked. d) The HBC620 channel is shown with transfected cells masked.

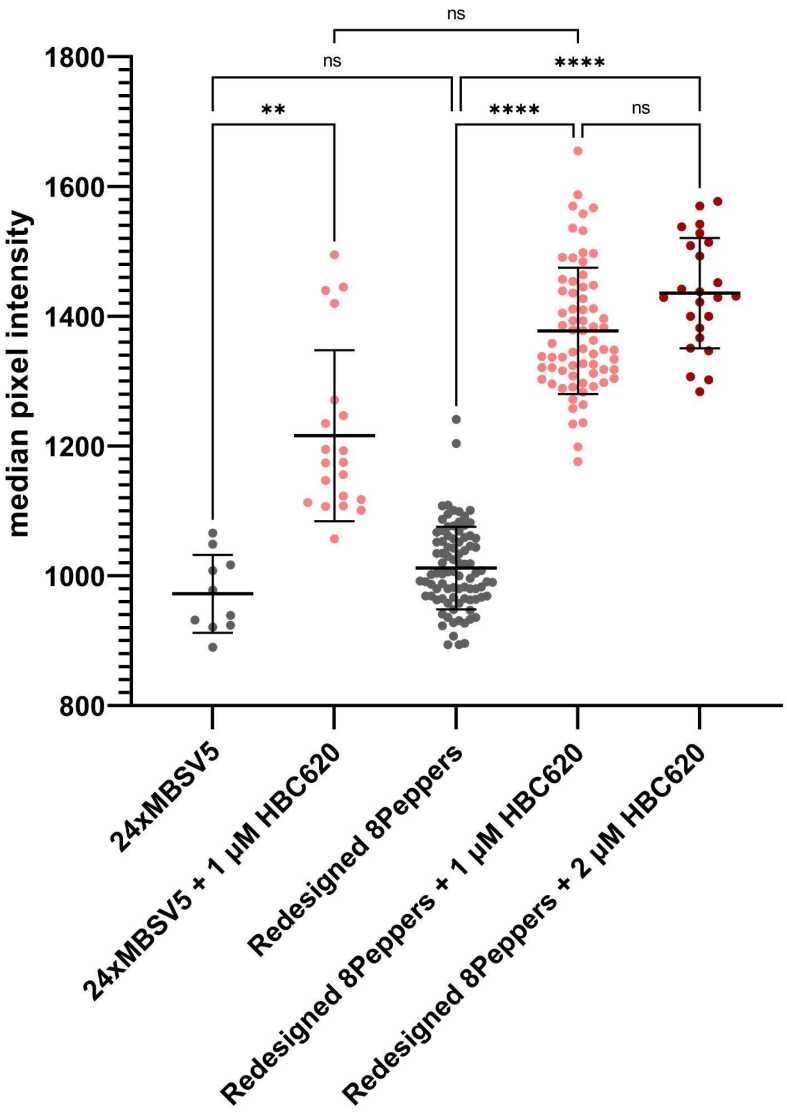

Figure 17: The whole cell median fluorescence intensity cell. Imaging was performed on a spinning disk confocal microscope using U2-OS cells with a NucBlu stain, JF646 for Halotag, and HBC620 for redesigned 8Peppers. The 24xMBSV5 array was used as a negative control for binding to HBC620. Statistical significance is present between conditions with and without probe. No statistical significance is seen between fluorescence intensity of probe binding the 24xMBSV5 and redesigned 8xPeppers array, even with varying probe concentrations.

The median values were used in figure 17 because high-intensity outliers caused the mean to be less representative of the data set. These could be due to dead cells where the probe

has aggregated or general cellular abnormalities that can't be controlled for. A one-way ANOVA with a Kruskal-Wallis statistical test was run because the data did not follow a gaussian distribution. The first experiment showed a significant difference between no probe and redesigned 8Peppers conditions, but no significance between redesigned 8Peppers and the negative control. This indicates the probe was not effectively binding the RNA aptamer. There also was not a significant difference between 1 μM and 2 μM probe concentrations indicating the probe effectively saturates the redesigned 8Peppers RNA at a 1 μM concentration, or doesn't bind at all.

In figure 17, the MS2 system showed a statistically significant intensity increase when probe was added. This negative control should not have been able to bind HBC620 and induce turn-on, which means HBC620 might be binding non-specifically or have a high background fluorescence. This visually correlates with the images seen in figure 16. The cells which were transfected do not visually appear brighter than cells that were not transfected.

The first experiment showed a 1.13 fold turn-on for redesigned 8Peppers. This was calculated by dividing the median of redesigned 8Peppers pixel intensity by MS2 median pixel intensity. Since the redesigned probe did not significantly outperform the negative control, I wanted to compare it to a positive control. After acquiring the WT 8Peppers plasmid, I could compare our redesigned 8Peppers to Chen et. al's imaging tool.

Figure 18 shows examples of each experimental condition in the second set of *in vivo* experiments. New HBC620 was used. It is unclear how stable HBC620 is in solution; one source says it is stable for 18 months in pure DMSO (Fluorescence Diagnosis (Shanghai) Biotech Co. Ltd., 2019) and another states it is not stable at all in the recommended solution of 10% DMSO, 40% PEG-300, 45% saline, and 5% Tween-80 ("HBC620: HBC Analog." Medchemexpress.). In

the original Peppers paper, Chen and coworkers do not elaborate on how HBC620 was prepared or stored for cellular use. Thus, a stock of HBC620 was prepared an hour before imaging to ensure the probe did not degrade.

WT 8Peppers had a different transfection marker because of time constraints with cloning issues. I attempted to clone the HaloTag β-actin gene into the pcsDNA-MCS-8Peppers plasmid, but didn't successfully create the product. Since there were time constraints, I used another transfection marker. The 488 nm excitation channel in figure 18 shows GFP labeled f-actin as a cytosolic marker for transfected cells. Both the marker and WT 8Peppers plasmid were transfected into cells at a 2:1 mass to mass ratio with the assumption that if the cell received the marker, it would likely uptake the WT 8Peppers plasmid.

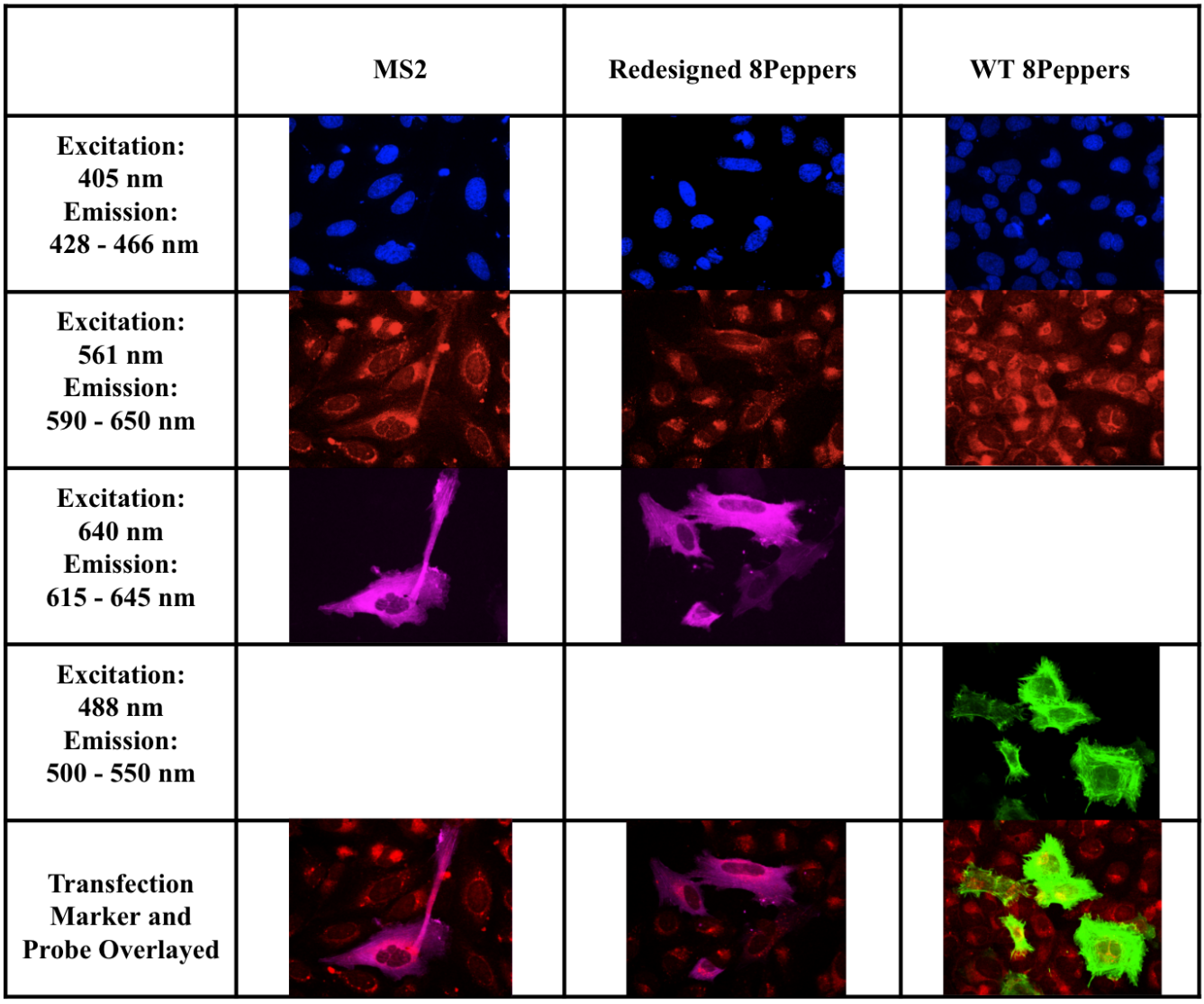

Figure 18: Examples of the imaging channels for each condition with 1 μM HBC620 from the second round of in vivo experiments. The 561 nm excitation channel shows the experimental channel stained with HBC620. The 640 nm and 488 nm excitation channels were used to determine transfection and for masking cells. The 405 nm excitation channel shows a nuclear marker. All images were taken in U-2 OS cells on a Nikon Spinning Disk Confocal microscope.

In figure 18, HBC620 stains the cell outside of the nucleus. The fluorescence is not uniform and diffuse. It appears to be localizing to the organelles surrounding the nucleus such as the rough endoplasmic reticulum or the Golgi apparatus. Similar to the first experiment, the cells

which were transfected do not seem visually brighter than untransfected cells around it. Figure 19 shows the quantitative analysis after masking transfected cells. The same image analysis and statistical test was done for experiment two as experiment one.

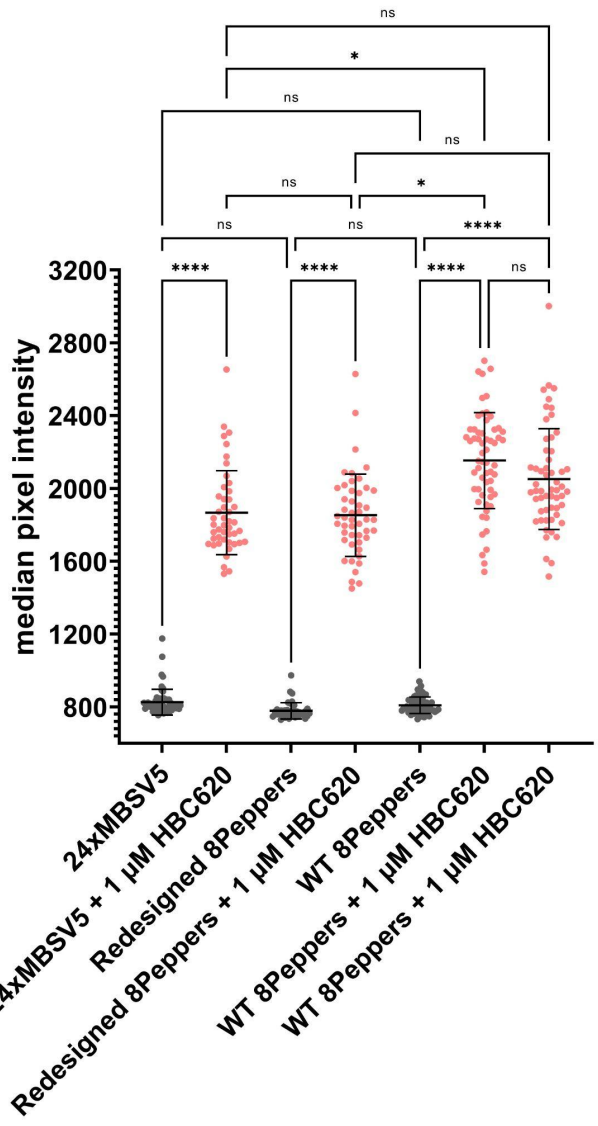

Figure 19: The whole cell median fluorescence intensity cell. Imaging was performed on a spinning disk confocal microscope using U2-OS cells with a NucBlu stain, JF646 for Halotag, GFP for LifeAct, and HBC620 for redesigned 8Peppers. The 24xMBSV5 array was used as a negative control for binding to HBC620. WT 8Peppers array was used as a positive control for binding to HBC620. Each dot represents an individual cell in one field of view in one imaging dish.

The comparisons between negative control, positive control, and redesigned 8Peppers to their respective no probe condition are statistically significant meaning there is an increase in fluorescence signal when adding probe. The negative control shows no difference in fluorescence intensity to redesigned 8Peppers. This is consistent with the first experiment. However, this time there is a decrease in fold intensity from redesigned 8Peppers to the MS2 system, indicating the negative control slightly outperformed the redesigned imaging tool at 0.98 fold decrease.

When comparing redesigned 8Peppers to the positive control, there is a significant increase as the WT 8Peppers outperformed redesigned 8Peppers in one dish. The first dish of WT 8Peppers shows about a 1.22 fold turn-on compared to redesigned 8Peppers and the negative control. The technical replicate does not show a significant difference. The increase in fluorescence intensity was not reproducible.

The second experiment confirms the redesigned 8Peppers cannot outperform a negative control and cannot induce fluorescence turn-on in HBC620. While the WT 8Peppers induces a slight increase in fluorescence intensity, it is inconsistent and not dramatically brighter than the negative control.

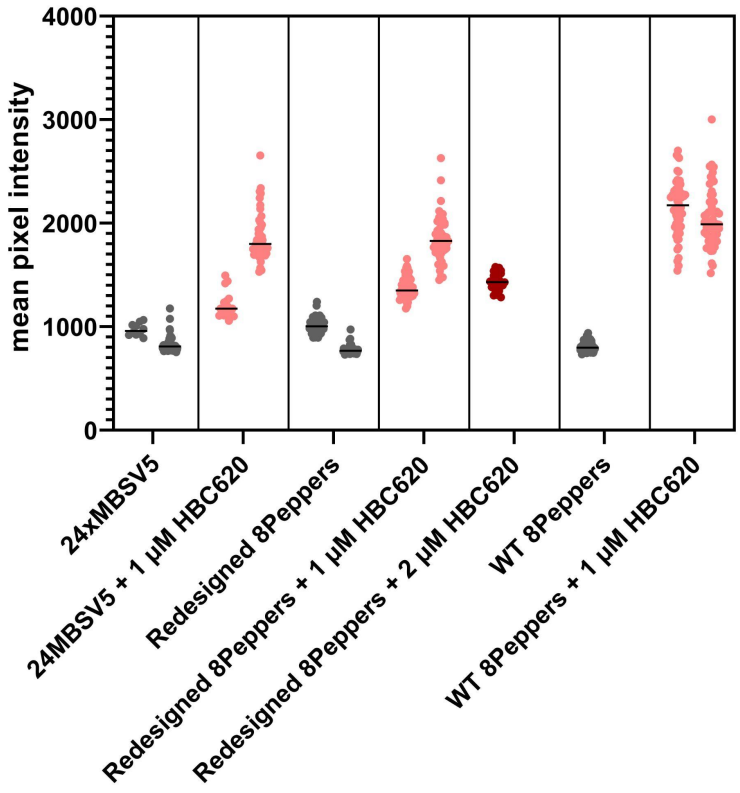

Figure 20: The combined data from imaging experiment one and two. Each column shows an experimental condition. Within the columns for MS2 and redesigned 8Peppers with two data sets, the first data set uses the old stock solution of HBC620 and the second uses the new stock solution of HBC620, thus comparing new versus old probe.

When directly comparing experiments one and two in figure 20, the second experiments showed a greater fluorescence turn-on in both the MS2 and redesigned 8Peppers condition. A two way nested ANOVA statistical test was run on all 591 cells reported. Looking at random effects, the average variation in median pixel intensity between conditions was 269.9. The average variation within a biological replicate of the same condition was 161.9.This means there was some variance between replicates of the same conditions. The P-value for investigating if the replicates differ is less than 0.0001. This means there is a large statistical significance

between replicates of the same experimental condition and the second experiment did have a brighter fluorescence intensity.

The two experiments also allow comparison of probe intensity under different conditions. The 1 μM probe of the second experiment had a higher fluorescence intensity than the 2 μM probe concentration of the first experiment. This could mean HBC620 quickly degrades in solution and is not stable as the first experiments used an older probe stock. However, the incubation times also changed between the conditions. The incubation time for the probe before imaging was not standardized in Chen and coworkers' paper. Thus, in the first experiment the probe was added immediately before imaging and in the second experiment the probe was incubated for 30 minutes to see if it helped demonstrate a difference between redesigned 8Peppers and the negative control. The change in incubation time or the freshness of the HBC620 stock solution could have both affected the fluorescence intensity.

Discussion

Redesigned Peppers does not outperform negative or positive controls

The overarching goal of this project was to redesign the RNA imaging tool, Peppers. I also aimed to validate Erin Richards' systematic pipeline of RNA imaging tool evaluation by following her protocol; this included live cell imaging, smFISH, and characterizing cellular perturbations. The rationale of the redesign was to make a more favorable folding pattern for the RNA to be synthesized in the native form more reliably. To achieve this, I created redesigned 8Peppers as an array of aptamers using the stem and linkers from the MS2 system with a series of synonymized Peppers aptamers. I set out to test the redesigned Pepper aptamer array both *in vitro* and in cells. *In vitro* experiments can provide information on whether the RNA can be

produced and whether it binds the ligand. On the other hand, *in vivo* experiments can provide information on whether the RNA is capable of binding and turning-on the ligand in cells and whether the fluorescence intensity is above the background fluorescence in the cell.

The *in vitro* tests of redesigned Peppers showed it did not produce the same fluorescence turn-on as WT Peppers. The fluorescence assay showed WT 1Peppers consistently produced a much higher fluorescence intensity than redesigned 1Peppers. For example, at 10 nM probe and 100 nM RNA, WT 1Pepper showed a 550-fold turn-on, whereas the redesign 1Pepper showed a 2.7-fold turn-on. Redesigned Peppers might bind the dye differently than WT Peppers, resulting in less effective fluorescence turn-on. Rigidification of the dye is what allows the dye to emit a photon and become fluorescent. If the RNA does not hold the dye still, the rotational and vibrational movement allows the dye to dissipate energy through motion rather than emitting a photon after excitation. Thus, a change in how the Peppers RNA binds the dye could alter the fluorescence intensity and potential for turn-on. It is also possible that the redesigned Peppers doesn't bind HBC620 with the same affinity and perhaps a much higher concentration of dye would be needed to saturate binding. The RNA aptamer might also not fold correctly. I knew I produced the RNA of the correct length from the denaturing gel, but I do not know if it was able to fold correctly. The experiments I completed don't allow me to distinguish between which of the reasons caused the fluorescence intensity to be less in redesigned Peppers. I could measure K_d via isothermal titration calorimetry to better understand how the RNA binds the dye, and even give clues to if the aptamer is folding correctly.

I also wanted to test 1Peppers, 4Peppers, and 8Peppers to observe fluorescence turn-on in varying repeats of aptamer. However, I was unable to produce 8Peppers RNA. I saw incomplete transcription products because the 8Peppers DNA produced a length of RNA similar to

4Peppers. I knew I created the 8Peppers DNA because I was able to clone it into Erin Richards' plasmid and it sequenced correctly. I could have an unexpected RNA polymerase termination site in the later portions of the sequence that causes the T7 polymerase to prematurely stop transcription. I would have to look at the sequence or change which polymerase I use. There could also be a GC rich area that causes the polymerase to de-attach and create a shorter product. I could adjust the temperature of the *in vitro* transcription reaction to accommodate for any GC rich regions (Grooms, 2022). I could also not have enough 8Peppers DNA for a template for the reaction. Since it was difficult to produce the DNA, I had scaled down the *in vitro* transcription reaction. One paper recommends doing a large scale *in vitro* transcription for highly repetitive sequences of RNA and purifying it via high performance liquid chromatography (HPLC) (Karlsson, et al., 2021); this helps increase the chance of creating the RNA of interest. I could have also lost the RNA during the gel purification step and purifying via HPLC would mitigate issues in purification. There are many future directions to optimize *in vitro* experiments to better understand redesigned Peppers binding and folding capabilities.

The redesigned 8Peppers, negative control of MS2, and positive control of WT 8Peppers performed similarly *in vivo*. One dish showed WT 8Peppers had a significant fluorescence intensity increase, but it was not reproducible. I was not able to get the same 8.5 - 11.0 fold turn-on as Chen and co workers for WT 8Peppers (Chen, et al., 2019). Other researchers report similar issues with WT 8Peppers. One paper shows that in live cell imaging, WT 8Peppers had a 1.2 fold turn-on (Bühler, et al., 2023). This is similar to my reported 1.13 fold turn-on of redesigned 8Peppers in the first imaging experiment. While the redesign does not produce noteworthy or reproducible results, neither does WT 8Peppers.

There are a few possible reasons why neither Peppers design performed well under cellular conditions. When an RNA is expressed in a cell, there are a number of factors that influence the amount of RNA present. RNA is produced by the process of transcription and the RNA polymerase needs to be able to synthesize the RNA. As mentioned previously, RNA folds co-transcriptionally and complicated or long repetitive sequences have a chance of mis-folding. Wu et al. showed that repeating units of RNA tend to have a high degree of heterogeneity of RNA (Wu, et al., 2015). I aimed to minimize this issue by synonymizing the 8Peppers sequence, however it is not clear if this helped. There could be issues in the transcription of the RNA where the cellular polymerase is not able to form the complete product for the same aforementioned reasons as *in vitro* transcription. The DNA sequence could also be unstable. Once the DNA has been transfected in the cell, the cell must replicate the DNA and repetitive sequences are prone to recombination or deletion (Byzmek and Lovett, 2021).

The Peppers RNA itself could also degrade under cytosolic conditions. Ribonucleases could be cleaving the RNA internally or hydrolyzing the RNA from the 3' or 5' ends (Housely and Tollervey, 2009). Processing-bodies, or p-bodies, are sites of mRNA decay and could be digesting the Peppers RNA (Luo, et al., 2018). RT-qPCR could be used to monitor the stability of Peppers RNA and quantify how much mRNA is present at different timepoints in the cell. This would tell me how stable the RNA is and if there is a significant decrease in Peppers RNA at any point under cytosolic conditions. With this information, I could plan imaging experiments closer or further from transfection to optimize the amount of Peppers RNA present in the cell.

How I made the probe for *in vivo* experiments could also affect its ability to bind the aptamer. HBC620 was suspended in a solution of PEG-300 and Tween-80 which are solubilizers that encase the probe. The bubble formed around HBC620 could impact its ability to enter into

cells. If the probe can't effectively enter the cell, this could explain why there was no difference in turn-on.

There are many reasons why WT 8Peppers and redesigned 8Peppers didn't exhibit a high fluorescence turn-on. However, the inability to reproduce the fluorescence intensity that Chen and coworkers found with WT Peppers illustrates the importance of having a systematic pipeline of evaluation for RNA imaging. A tool should be dependable and able to reproduce high quality data. Hence, a rigorous evaluation is necessary for all RNA imaging tools.

Comparison of redesigned 8Peppers to iPeppers

Inert Peppers (iPeppers) was introduced by Wang et al., and also aimed to restructure Peppers RNA imaging system. They used a tandem array of inert Peppers that folded only when bound to HBC530 and target RNA sequence. Their lab also took WT 1Peppers, synonymized parts of the structure, and created a linker sequence between repeating units. Their system differs from redesigned 8Peppers in that it is not genetically encoded and cannot fold independently of a template RNA to bind to. However, some of their structural findings can be discussed with respect to redesigned 8Peppers (Wang, et al., 2022).

Wang and coworkers found that the stem loop of one Pepper aptamer greatly affected its folding capabilities. They found that HBC binding stopped when the stem was less than four nucleotides; the intramolecular hydrogen bonds were destabilized with three or less nucleotides in the stem. They experimented up to six base pairs, but established that folding of the aptamer is influenced by the stem and its length (Wang, et al., 2022). On my redesigned 8Peppers structure, the MS2 linkers also included stems, thus the original three nucleotide stem was removed. The MS2 stems were seven nucleotides long and synonymized (Tutucci, et al., 2018 (1)). Working

with Dr. Palmer and Dr. Batey, we hypothesized the length of the stem could affect HBC620 binding and this might contribute to the performance of redesigned Peppers. To optimize redesigned Peppers, it could be beneficial to use the original three nucleotide stem and test longer variations up to six nucleotides.

The general folding capabilities of this RNA are also not consistent in Wang et al.'s paper. Although their system was designed differently, it still included a series of Peppers aptamers separated by linkers. This paper showed iPeppers gained a functional structure and activated fluorescence when bound to target RNA. Thus, iPeppers was designed to remain inert until bound to target RNA, instead of folding independently (Wang, et al., 2022). Redesigned Peppers is not designed to bind to a target RNA, but can still have some of the *in vitro* folding issues Wang and coworkers elucidated.

Both the original Peppers and iPeppers papers showed that eight repeating units had the best signal to noise ratio and fluorescence intensity (Wang, et al., 2022) (Chen, et al., 2019). Due to the poor fluorescence turn-on and inability to produce the 8Pepper redesign aptamer in vitro, I was unable to test the fluorescence turn on of 1Pepper, 4Pepper and 8Pepper, although it is reasonable to predict that an increase in the number of aptamers could increase the fluorescence intensity.

Wang and coworkers' iPeppers provides a similar structure and purpose to redesigned Peppers. This made it a good point of comparison for trouble-shooting the performance of redesigned 8Peppers.

Future Directions

The data I collected provided an overview of redesigned Peppers and WT Peppers. However, more experiments and optimization are required to truly understand the limitations and patterns of each imaging tool. The first step is to optimize imaging conditions to try to reproduce the 8.5-11.0 fold fluorescence turn-on in live cell imaging reported by Chen and coworkers. I would begin by synthesizing the WT 8Peppers plasmid with a HaloTagged β-actin gene. This would allow me to know that the cell received and produced the WT 8Peppers aptamer; if the cell has gone through transcription and translation of the HaloTagged β-actin gene, then it is also producing the RNA of interest.

The HBC620 usage needs to be optimized. I saw enhanced results when the probe was suspended in solution within an hour of imaging and then incubated for thirty minutes prior. Bühler and coworkers reported incubating HBC620 with WT 8Peppers for two hours prior to imaging (Bühler, et al., 2023). I would like to optimize the incubation time and test the shelf stability of HBC620. I currently have an aliquot of dye at room temperature to check its structure via high-performance liquid chromatography (HPLC).

WT 8Peppers and redesigned 8Peppers could be tested on various microscopes. Chen's lab showed that a two photon microscope and confocal microscope produced similar results. The camera varies between microscopes and some could have a different level of sensitivity. The intensity of the laser power would also affect the fluorescence intensity. I set the laser power to 15% when using 561 nm excitation for HBC620. While this is a relatively low power, it could be causing the fluorophore to photobleach. I could also reduce the laser power and try a different exposure setting to minimize potential effects of photobleaching. I would also test various cell lines such as HeLa and Cos-7 cells used in Chen's paper (Chen, et al., 2019). Each cell line

expresses enzymes at different levels and can have varying concentrations of cytosolic metals. These two factors associated with cell lines could affect the production and folding of RNA. Identifying the best combination of cell type, microscope, and HBC620 usage could improve the fluorescence intensity of the two Peppers designs.

More *in vitro* experiments could also be performed to optimize redesigned 8Peppers. Chen's paper showed that fluorescence intensity increased up to 8 repeats of Peppers and did not improve signal to noise ratio past 8 repeats (Chen, et al., 2019). I would like to test redesigned 1Peppers, 4 Peppers, and 8Peppers in a fluorescence assay to determine whether changes in the number of repeats influences fluorescence intensity. For these experiments, I think it will be important to vary either the RNA or the probe concentration in order to test whether the K_D of the Pepper aptamer was altered by redesign.

After optimizing redesigned 8Peppers and WT 8Peppers, I would like to continue to follow Erin Richards' systematic pipeline of evaluation. The tools should be characterized via single molecule Fluorescence In Situ Hybridization (smFISH) in order to quantify colocalization of the aptamer array with the RNA to which it is attached. As mentioned previously, Wu et al showed that highly repetitive sequences led to a decrease in colocalization, either due to recombination and deletion or degradation. It is expected that this problem would be mitigated by synonymization. However, whether the WT 8Pepper design suffers from low colocalization and heterogeneity in the integrity of the RNA has not been tested. smFISH would also enable characterization of cytosolic versus nuclear localization to evaluate whether the RNA tag alters processing and localization of the RNA.

Finally, there is a possibility that attachment of an array of aptamers to an RNA of interest could perturb expression, half-life and function of that RNA. Therefore it would be

critical to check for these perturbations. A western blot would be done to assess the tool's effect on protein production and RT-qPCR would be done to assess its effect on mRNA expression level. This would allow a greater understanding of the benefits and limitations of each probe and shine a light onto how to best construct an RNA imaging tool. It would reveal if a cell can truly produce an extremely long hairpin loop or if many shorter synonymized loops are favorable.

Conclusion

RNA imaging tools have proven to be a necessary component of RNA research. These tools allow scientists to track where and when RNA localizes within the cell and can be used in biological studies to understand the function of RNA. It is important to optimize current tools and create innovative and dependable new tools. It is also important to characterize how RNA imaging tools affect cellular function and be able to predict perturbations. This allows scientists to conduct a more informed data analysis.

As the field of RNA imaging improves, new tools and optimized old tools will appear. In this paper, I attempted to redesign and improve the existing Peppers RNA imaging platform. I completed a redesign that incorporated features from the MS2V6 system. This redesign was tested *in vitro* to assess binding to the HBC620 ligand. Redesigned 1Peppers had a much weaker fluorescence intensity than WT 1Peppers, indicating the alterations to the nucleotide sequence negatively affected the ability of the aptamer to turn on HBC620 fluorescence.

Redesigned 8Peppers was tested in U-2 OS cells, with the MS2 system as a negative control and WT 8Peppers as a positive control. I expected the MS2 to not show an increase in fluorescence intensity as it is not constructed to bind to HBC620. I also expected WT 8Peppers to bind HBC620 and initiate fluorescence turn-on. Neither of these predictions occurred and all

three conditions performed similarly. WT 8Peppers had a slight increase in fluorescence intensity compared to the MS2 system and redesigned 8Peppers, however it was not reproducible. Either the imaging conditions could be optimized or both of Peppers imaging systems are not reliable.

There are many avenues for improvement and further optimizations can be done to improve redesigned Peppers. These experiments also showed the necessity of having standardized protocols for characterizing RNA imaging tools. The tools broadly appear to have varying performance when used by different labs; the signal-to-noise ratios and fluorescence intensity should be known and reproducible so conclusions are not being drawn from variable data. Most RNA imaging tools also have unknown effects on cellular health, which can perturb RNA activity. The field of RNA imaging holds promise for understanding more about RNA behavior and its effect on certain medical conditions, but needs reliable tools to do so. As the field continues to grow and improve, quality assurance will be a must for imaging tools.

Acknowledgements

This project could not have happened without the endless support of the Palmer Lab. First and foremost, I would like to thank Erin Richards and Logan McCoy for their expertise and guidance. They were always willing to spend extra hours helping me with my project, answering questions, and giving me guidance on papers, classwork, and life itself. I can't thank them enough. I would also like to thank Dr. Amy Palmer for her mentorship throughout my undergraduate research journey. She is an inspiring mentor for me and I am grateful for her support in making me a new scientist. I would like to extend my gratitude to Dr. JulieMarie Shepherd Macklin for agreeing to be a committee member on a field outside her study and Dr. Jeff Cameron for aiding in my thesis.

Dr. Rob Batey and Shelby Lennon helped me design my project and coach me through *in vitro* experiments. I would like to thank them for their time and letting me use their lab. Thank you to Aleksandra Weirzba for your help along the way.

I also had the opportunity to grow my skills abroad and would like to thank the Laboratory of Experimental Biophysics at EPFL in Switzerland. Thank you to Dr. Suliana Manley for hosting me. Thank you to Julius Winters for helping me become a more independent and confident researcher, while honing in live-cell microscopy skills.

Thank you to the Undergraduate Research Opportunities Program (UROP) for funding a portion of my thesis and the Think Swiss Scholarship for giving me the opportunity to extend my science experience abroad.

References

Berg, Jeremy M., et al. *Biochemistry*. 9th ed., MacMillan Learning, 2019.

Biochemistry, RNA Structure - StatPearls - NCBI Bookshelf.

https://www.ncbi.nlm.nih.gov/books/NBK558999/.

Bourke, Ashley, et al. "Decentralizing the Central Dogma: mRNA Translation in Space and

Time." *Molecular Cell*, Cell Press, 19 Jan. 2023,
https://www.sciencedirect.com/science/article/pii/S1097276522012138.

Braselmann, Esther, et al. "A Multicolor Riboswitch-Based Platform for Imaging of RNA in Live Mammalian Cells." *Nature News*, Nature Publishing Group, 30 July 2018,
https://www.nature.com/articles/s41589-018-0103-7.

Braselmann, Esther, et al. "Illuminating RNA Biology: Tools for Imaging RNA in Live

Mammalian Cells." *Cell Chemical Biology*, U.S. National Library of Medicine, 20 Aug. 2020, https://pubmed.ncbi.nlm.nih.gov/32640188/.

Bühler, Bastian, et al. "Avidity-Based Bright and Photostable Light-up Aptamers for

Single-Molecule MRNA Imaging." *Nature News*, Nature Publishing Group, 19 Jan. 2023, https://www.nature.com/articles/s41589-022-01228-8.

Bühler, Bastian, et al. "Bright, Fluorogenic and Photostable Avidity Probes for RNA Imaging." *BioRxiv*, Cold Spring Harbor Laboratory, 1 Jan. 2021,
https://www.biorxiv.org/content/10.1101/2021.11.02.466936v1.

Byzmek, Malgorzata, and Susan Lovett. "Instability of Repetitive DNA Sequences: The Role of

Replication in Multiple Mechanisms." *PNAS*, 17 July 2021,
https://www.pnas.org/doi/10.1073/pnas.111008398.

Cawte, Adam D., et al. "Live Cell Imaging of Single RNA Molecules with Fluorogenic Mango II

Arrays." *Nature News*, Nature Publishing Group, 9 Mar. 2020, https://www.nature.com/articles/s41467-020-14932-7.

Chen, Xianjun, et al. "Visualizing RNA Dynamics in Live Cells with Bright and Stable Fluorescent RNAS." *Nature News*, Nature Publishing Group, 23 Sept. 2019, https://www.nature.com/articles/s41587-019-0249-1.

Garcia, Jennifer, and Roy Parker. "MS2 Coat Proteins Bound to Yeast MRNAs Block 5′ to 3′ Degradation and Trap MRNA Decay Products: Implications for the Localization of MRNAs by MS2-MCP System." *RNA Society*, Cold Spring Harbor Lab, 28 May 2015, https://rnajournal.cshlp.org/content/21/8/1393.long.

Grooms, Kelly. "In Vitro Transcription: Common Causes of Reaction Failure." *Promega Connections*, 16 Sept. 2022, https://www.promegaconnections.com/in-vitro-transcription-common-causes-of-reaction-failure/.

"HBC620: HBC Analog: Medchemexpress." *MedchemExpress.com*, https://www.medchemexpress.com/hbc620.html.

Hetherington, Lisa. "What Is RNA." *RNA Society*, https://www.rnasociety.org/what-is-rna.

Housely, Jonathan, and David Tollervey. "The Many Pathways of RNA Degradation." *Cell*, 20 Feb. 2009, https://www.cell.com/fulltext/S0092-8674(09)00067-1.

"How Do Different Types of Covid-19 Vaccines Work?" *Mayo Clinic*, Mayo Foundation for Medical Education and Research, 25 Aug. 2022, https://www.mayoclinic.org/diseases-conditions/coronavirus/in-depth/different-types-of-covid-19-vaccines/art-20506465.

"How to Design a Primer." *Addgene*, h*ttps://www.addgene.org/protocols/primer-design/.*

Huang, Kaiyi, et al. “Structure-based investigation of fluorogenic Pepper aptamer.” Nature Chemical Biology, 1 November 2021, https://www.nature.com/articles/s41589-021-00884-6

Johansson, Hans E., et al. “RNA Recognition by the MS2 Phage Coat Protein.” *Seminars in Virology*, Academic Press, 25 May 2002, https://www.sciencedirect.com/science/article/abs/pii/S1044577397901207?via%3Dihub.

Karlsson, Hampus, et al. “Production of Structured RNA Fragments by In Vitro Transcription and HPLC Purification.” *Current Protocols*, 17 June 2021, https://currentprotocols.onlinelibrary.wiley.com/doi/full/10.1002/cpz1.159.

Leamy, Kathleen A., et al. “Bridging the Gap between in Vitro and in Vivo RNA Folding.” *Cambridge Core*, Cambridge University Press, 24 June 2016, https://www.cambridge.org/core/journals/quarterly-reviews-of-biophysics/article/bridging-the-gap-between-in-vitro-and-in-vivo-rna-folding/212048535F57656F96376B82DA31F.

Lewis, Mark W. et al. “Predicting 3D RNA Folding Patterns via Quadratic Binary Optimization.” *ArXiv abs/2106.07527* (2021): n. pag.

Luo, Yang, et al. “P-Bodies: Composition, Properties, and Functions .” *ACS Publications*, 30 Jan. 2018, https://pubs.acs.org/doi/10.1021/acs.biochem.7b01162.

Mathis, Stéphane, and Gwendal Le Masson. “RNA-Targeted Therapies and Amyotrophic Lateral Sclerosis.” *Biomedicines*, U.S. National Library of Medicine, 15 Jan. 2018, https://www.ncbi.nlm.nih.gov/pmc/articles/PMC5874666/.

Miller, Nicole. “The Mysteries of RNA.” *Grow: Wisconsin's Magazine for Life Sciences*, 2014, https://grow.cals.wisc.edu/.

Fluorescence Diagnosis (Shanghai) Biotech Co. Ltd. *Pepper Fluorescent RNA Technology: Enabling Background Free Imaging of RNAs in Live Cells*, 2019.

"RNA Biology." *National Institutes of Health*, U.S. Department of Health and Human Services, https://irp.nih.gov/our-research/scientific-focus-areas/rna-biology.

Strack, Rita L, and Samie R Jaffrey. "Live-Cell Imaging of Mammalian RNAS with spinach2." *Methods in Enzymology*, U.S. National Library of Medicine, 2015, https://www.ncbi.nlm.nih.gov/pmc/articles/PMC4382203/.

(1) Tutucci, Evelina, et al. "An Improved MS2 System for Accurate Reporting of the Mrna Life Cycle." *Nature Methods*, U.S. National Library of Medicine, Jan. 2018, https://www.ncbi.nlm.nih.gov/pmc/articles/PMC5843578/.

(2) Tutucci, Evelina, et al. "Single-Mrna Detection in Living S. Cerevisiae Using a Re-Engineered MS2 System." Nature News, Nature Publishing Group, 14 Sept. 2018, *https://www.nature.com/articles/s41596-018-0037-2*.

Vera, Maria, et al. "Imaging Single Mrna Molecules in Mammalian Cells Using an Optimized MS2-MCP System." *Springer Nature Experiments*, 13 Aug. 2019, https://experiments.springernature.com/articles/10.1007/978-1-4939-9674-2_1.

Wang, Qi, et al. "Inert Pepper aptamer-mediated endogenous mRNA recognition and imaging in living cells." *Nucleic Acids Research*, 17 May 2022, https://pubmed.ncbi.nlm.nih.gov/35580055/

Wu, Bin, et al. "Synonymous Modification Results in High-Fidelity Gene Expression of Repetitive Protein and Nucleotide Sequences." *Genes & Development*, Cold Spring Harbor Lab, 18 Mar. 2015, http://genesdev.cshlp.org/content/29/8/876.full.

Yang, Liang-Zhong, et al. "Dynamic Imaging of RNA in Living Cells by CRISPR-Cas13 Systems." *Molecular Cell*, Cell Press, 19 Nov. 2019, https://www.sciencedirect.com/science/article/pii/S1097276519308020.

Zaepfel, Benjamin L., and Jeffrey D. Rothstein. “RNA Is a Double-Edged Sword in ALS Pathogenesis.” *Frontiers*, Frontiers, 22 June 2021, https://www.frontiersin.org/articles/10.3389/fncel.2021.708181/full.

Zemora and Waldsich. “RNA Folding in Living Cells.” *RNA Biology*, U.S. National Library of Medicine, 2010, https://www.ncbi.nlm.nih.gov/pmc/articles/PMC3073324/.

Supplementary

Supplementary Table 1: WT 1Peppers Aptamer without Three Nucleotide Stem

CCAAUCGUGGCGUGUCGGCCUGCUUCGGCAGGCACUG GCGCCG	Source: Chen, et al., 2019

Supplementary Table 2: Redesigned 8Peppers with 50 nucleotide linker

ACCGGTAACCTACAAGCTCAGCAACATGCGCAATCGTGC GGTGTCGGTCTGCGCGAGCAGACACTGGCCGCCGCATGC ATGGTGCAGAATATCGGCATGTCTACTCGTACAGTCAAAT CTACTCGTGTGGTCGCAATCGTGTGGTGTCGGCGTACGT AAGTACGCACTGGCCACCGACCACTTCTATTCTATTCATC TTTTCGGTTGTGCAGGTATTCTGCCGATGTACGAGAAGCC AATCGTAGGGTGTCGGCCAACGTGAGTTGGCACTGGCCC TGCTTCTCGACTACCTTCATCATACATGGTGTGCAGATGG CCGCCAAGTTTTTTGCCAATGGGCAATCGTACGGTGTCG GCTCGCTCCGGCGAGCACTGGCCGTCCCATTCTCTGTCA ACCAACCCATGCAAAGTTTACACTCTGCTATGGCAGCAC TGTCGCAGCCAATCGTGTCGTGTCGGACAGCTATGGCTG TCACTGGCGACGCTGCGAGCCAAAACGGCCCCCGGTGC GTGTATTGCATCTGCCTTGCGAGCATTCACAGGGCCAATC GTGGAGTGTCGGTCAGCTGTGGCTGACACTGGCTCCGCC CTGCCGTTGCATTACTTCAATATGGGTGCTCTGTCGTCGT CATCAGGACCATTTGCGCGCAATCGTAACGTGTCGGCCT GCTTCGGCAGGCACTGGCGTTCGCGCATATATCATCAGC ACTCGTGCGGATACTTCTGGGATTCCTATTGTTACGCGAG CTCCCAATCGTACAGTGTCGGCATGCGCAAGCATGCACT GGCTGTGGAGCTCTGGCGACAGAGACCCTCACACGAGA TCTCATACGCGT	Source: Dr. Rob Batey, Dr. Amy Palmer, and Caitlyn Mendik Comments: 50 nucleotide linker Peppers 1 Peppers 2 Peppers 3 Peppers 4 Peppers 5 Peppers 6 Peppers 7 Peppers 8

Supplementary Table 3: 8 Synonymized Peppers Sequences

1) CATGCGCAATCGTGCGGTGTCGGTCTGCGCGAGCAGACA CTGGCCGCCGCATG 2) TGGTCGCAATCGTGTGGTGTCGGCGTACGTAAGTACGCAC TGGCCACCGACCA 3) AGAAGCCAATCGTAGGGTGTCGGCCAACGTGAGTTGGCA CTGGCCCTGCTTCT	Source: Dr. Rob Batey, Dr. Amy Palmer, and Caitlyn Mendik

4) AATGGGCAATCGTACGGTGTCGGCTCGCTCCGGCGAGCA CTGGCCGTCCCATT 5) CGCAGCCAATCGTGTCGTGTCGGACAGCTATGGCTGTCAC TGGCGACGCTGCG 6) CAGGGCCAATCGTGGAGTGTCGGTCAGCTGTGGCTGACA CTGGCTCCGCCCTG 7) TGCGCGCAATCGTAACGTGTCGGCCTGCTTCGGCAGGCA CTGGCGTTCGCGCA 8) AGCTCCCAATCGTACAGTGTCGGCATGCGCAAGCATGCA CTGGCTGTGGAGCT	